Elliptic triangle groups in $PU(2,1)$, Lagrangian triples and momentum maps

Julien Paupert
Institut de Mathématiques
Université Pierre et Marie Curie
4, place Jussieu
F-75252 Paris
e-mail: paupert@math.jussieu.fr

April 25, 2006

Abstract

We determine the possible eigenvalues of elliptic matrices A, B, C in $PU(2,1)$ satisfying $ABC = 1$. This is done by describing geometrically the image of a certain momentum map for the (non-compact) group action of $PU(2,1)$ by conjugation on $C_1 \times C_2$ where C_1 and C_2 are fixed elliptic conjugacy classes in $PU(2,1)$. Surprisingly, this image is not always convex, rather it is the union of one, two or three convex polygons in $\mathbb{T}^2/\mathfrak{S}_2$. The main motivation was to analyse elliptic triangle groups in $PU(2,1)$ such as Mostow's lattices.

Contents

1 Introduction

What we call an *elliptic triangle group* in $PU(2,1)$ is a subgroup generated by two elliptic elements A and B such that the product AB is elliptic. We address in this paper the following question: in such a group, what are the possible conjugacy classes for the product AB when A and B are each in a fixed conjugacy class?

It is a classical problem in a linear group to characterize the possible eigenvalues of matrices $A_1, ..., A_n$ satisfying $A_1 ... A_n = 1$. In the group $GL(n, \mathbb{C})$, this question, known as the Deligne-Simpson problem, has arisen from the study of so-called Fuchsian differential systems on Riemann's sphere $\mathbb{C}P^1$ and is closely related

to the Riemann-Hilbert problem (Hilbert's 21^{st} problem); see [Ko] for a survey of these questions and the partial answers which are known so far. The antipodal case of the compact group $U(n)$ has also been extensively studied and essentially solved in [AW], [Be], [Bi2], [Kl1]; it is related to many surprising branches of mathematics as is pointed out in the surveys [F] and [Kl2]. The case of $U(n)$ is also studied in relation with Lagrangian subspaces and reflections of $\mathbb{C}^n$ in [FW1], from which we have adapted some ideas to the setting of the non-compact group $PU(2,1)$.

Recall that an elliptic conjugacy class in $PU(2,1)$ is characterized by an unordered pair of angles (see [P] pp. 29–30); our question amounts to investigating the image in the surface $\mathbb{T}^2/\mathfrak{S}_2$ of the group product map restricted to a product $C_1 \times C_2$ of two conjugacy classes. This map is an example of a momentum map on the quasi-Hamiltonian space $C_1 \times C_2$, as defined in [AMM], which is a group-valued generalization of classical (Lie algebra-valued) momentum maps associated to Hamiltonian group actions on a symplectic manifold. We will not use this structure in the course of the proofs, and no knowledge of it is necessary.

We describe the image of this momentum map $\tilde{\mu}$ (see section 2.2 for a precise definition of $\tilde{\mu}$), and answer the related question of classifying triples of pairwise intersecting Lagrangian subspaces of $H^2_{\mathbb{C}}$ (or $\mathbb{R}$-planes). The image turns out to be the union of at most three (possibly overlapping) convex polygons in the surface $\mathbb{T}^2/\mathfrak{S}_2$. In particular it is not always convex (and not even locally convex when the different polygons overlap).

Our description of the image can be summarized by the two following results; note that in practice our criteria allow a complete determination of this image for two given elliptic conjugacy clases C_1 and C_2. Various examples of these image polygons were described and drawn in the last chapter of [P] (pp. 137–141).

We will denote by $W_{red} \subset \mathbb{T}^2/\mathfrak{S}_2$ the image of all reducible groups (in the sense of linear representations); each line segment of W_{red} will be called a *wall*. The complete description of this reducible framework occupies section 2.3. Now W_{red} **together with the two axes** $\{0\} \times S^1$ **and** $S^1 \times \{0\}$ disconnect $\mathbb{T}^2/\mathfrak{S}_2$ into a union of open convex polygons which we will call *chambers* (see section 2.5 for the appropriate notion of convexity). We will also call *totally reducible vertices* the two points which are the image of pairs (A, B) generating an Abelian group (i.e. having a common basis of eigenvectors).

Theorem 1.1 *Let C_1 and C_2 be two elliptic conjugacy classes in $PU(2,1)$, at least one of which is not a class of complex reflections. Then the image of the map $\tilde{\mu}$ in $\mathbb{T}^2/\mathfrak{S}_2$ is a union of closed chambers, containing in a neighborhood of each totally reducible vertex the convex hull of the reducible walls containing that vertex.*

This is reminiscent of the result of Atiyah-Guillemin-Sternberg (see [A], [GS1], [GS2]), knowing that in this case reducible groups are what come closest to fixed points under the action of $PU(2,1)$ by conjugation (they have the smallest orbits).

Concerning the hypothesis on C_1 and C_2, it is easily seen that two complex reflections always generate a reducible group because their mirrors (fixed $\mathbb{C}$-planes) intersect in $\mathbb{C}P^2$, so in that case the image is a non-convex union of segments (see figure 4.12 of [P]).

The second result can be stated as follows, but it is based on explicit obstructions for certain chambers to be full, notably the three corners of the half-square as well as all chambers touching the diagonal.

Theorem 1.2 *Let C_1 and C_2 be two elliptic conjugacy classes in $PU(2,1)$, corresponding to angle pairs $\{\theta_1, \theta_2\}$ and $\{\theta_3, \theta_4\}$, with $\theta_i \in [0, 2\pi[$, $\theta_1 \geqslant \theta_2$ and $\theta_3 \geqslant \theta_4$. Let:*

$$\tilde{\mu} : (C_1 \times C_2) \cap \mu^{-1}(\{\textit{elliptics}\}) \xrightarrow{\mu} G \xrightarrow{\pi} \mathbb{T}^2/\mathfrak{S}_2$$

be the associated momentum map. Then:

$$\tilde{\mu} \text{ is onto} \iff \begin{cases} \theta_1 - 2\theta_2 + \theta_3 - 2\theta_4 \geqslant 2\pi \\ 2\theta_1 - \theta_2 + 2\theta_3 - \theta_4 \geqslant 6\pi \end{cases}$$

The last section is devoted to a detailed study of the example which motivated this work, where the generators A and B have angle pairs $\{0, 2\pi/3\}$ and $\{2\pi/3, -2\pi/3\}$. This corresponds to generators for Mostow's lattices $\Gamma(3,t)$ defined in [M1]. The image is in that case a triangle, inside of which the family considered by Mostow is a segment going from one side to the other, see figures 12 and 15 (the lattices comprise 8 points inside this segment). The geometric impression is clear: it would be very surprising not to find other discrete groups (hopefully some nonarithmetic lattices) inside this picture; this will be further investigated in [PP].

Figure 1: A configuration of reducibles

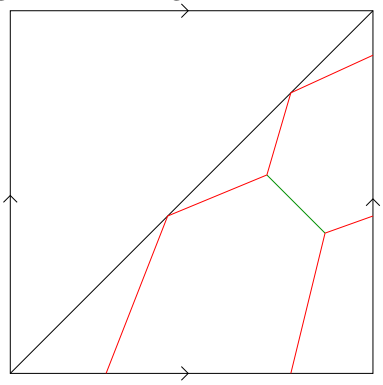

Acknowledgements: The author would like to thank Elisha Falbel, Richard Wentworth and Yves Benoist for useful discussions, as well as Frédéric Paulin and John Parker for many corrections and suggestions.

2 Elliptic triangle groups, a polygon of configurations

2.1 Introduction

In this section we describe the image of our momentum map $\tilde{\mu}$ in the surface $\mathbb{T}^2/\mathfrak{S}_2$ (see section 2.2 for a precise definition of $\tilde{\mu}$). We first describe in detail the collection of reducible points (in the sense that these are the images of pairs (A, B) which generate a reducible linear group), the main idea being that irreducible points project to interior points of the image, so that the image will be a union of the *chambers* bounded by the *reducible walls* (we will make these terms precise later on).

Reducible groups are here of two types, according to whether the fixed point of the action is inside or outside of complex hyperbolic space (it cannot be on the boundary if the generators are elliptic). When the fixed point is inside complex hyperbolic space, the group $\Gamma = \langle A, B\rangle$ is conjugate to a subgroup of $U(2)$ which is the stabilizer of a point in $PU(2,1)$; in that case we will say that Γ is *spherical reducible*. When the fixed point is outside complex hyperbolic space, the group $\Gamma = \langle A, B\rangle$ is conjugate to a subgroup of $P(U(1) \times U(1,1))$ which is the stabilizer of a complex geodesic, or $\mathbb{C}$-plane; in that case we will say that Γ is *hyperbolic reducible*. There are two special points which are both spherical reducible and hyperbolic reducible: these are the points where Γ is Abelian (in other words the two matrix generators have a common basis of eigenvectors). We will call these two groups *totally reducible*.

The image of all these reducible groups in $\mathbb{T}^2/\mathfrak{S}_2$ is then a trivalent graph with two vertices, with the following properties (which we will prove in section 2.3). The two vertices are the images of the two totally reducible groups. They are joined by a line segment of slope -1 which is the image of the spherical reducible groups. Two other segments emanate from each vertex, one of slope 2 and the other of slope $1/2$ corresponding to the two hyperbolic reducible families containing the vertex. Note that the slope of a line is well defined in the torus, but is only defined up to inversion in the quotient $\mathbb{T}^2/\mathfrak{S}_2$. Here we will use once and for all the same affine chart for $\mathbb{T}^2/\mathfrak{S}_2$, namely the lower half of the square, as in figure 1. Note that the sides of the square in this chart have a geometric meaning (in other words, the torus is not homogeneous) because they correspond to special conjugacy classes. In fact there is a subtlety because a point on one of these sides can represent two distinct conjugacy classes, one comprising $\mathbb{C}$-reflections (i.e. elliptic elements fixing a $\mathbb{C}$-plane) and the other parabolic transformations; these two classes are indistinguishable from the point of view of angles or trace (compare with Goldman's triangle in the complex plane of traces on pp. 204–205 of [G]; see also chapter 1). This ambiguity is greater at the three vertices of the triangle (all identified in the quotient) which represent the identity and all unipotent isometries (these are the Heisenberg translations on the boundary $\partial H^2_{\mathbb{C}} = H^3$).

2.2 The group product: a group-valued momentum map

The setting is that of the group $G = PU(2,1)$ which is a real semisimple Lie group, connected but not simply-connected, and non compact (more precisely, with real rank one). Each of these characteristics has its importance in the study of the momentum map which we now introduce. The most basic feature of this Lie group is its group product; in our setting, we are interested in the behavior (principally, the image) of this map restricted to a product of two fixed conjugacy classes. More precisely, let C_1 and C_2 be two conjugacy classes of elliptic elements in $PU(2,1)$; we consider the map:

$$\begin{array}{rccc} \mu: & C_1 \times C_2 & \longrightarrow & G \\ & (A,B) & \longmapsto & AB \end{array}$$

$C_1 \times C_2$ is a typical example of a quasi-Hamiltonian G-space (the G-action being by conjugation on each factor), as defined in [AMM] (see also chapter 4 of [Sf] for more details) with an associated group-valued momentum map which is simply the product μ. The classical notion of a momentum map associated with a Hamiltonian group action on a symplectic manifold can be found for instance in [W2], with a survey of different directions of generalization.

In fact, we are only concerned here with the conjugacy class of the product and we restrict ourselves to the case when this product is elliptic, so that we consider the map:

$$\tilde{\mu} : (C_1 \times C_2) \cap \mu^{-1}(\{\text{elliptics}\}) \xrightarrow{\mu} G \xrightarrow{\pi} \mathbb{T}^2/\mathfrak{S}_2$$

where π denotes the projection from G to the set of its conjugacy classes (recall that an elliptic conjugacy class in $PU(2,1)$ is characterized by, and identified to, an unordered pair of angles, see chapter 1 of [P]). Note that we might have lost the quasi-Hamiltonian structure by restricting μ to $\mu^{-1}(\{\text{elliptics}\})$; however when this structure is needed we can restrict a bit more, to $\mu^{-1}(\{\text{regular elliptics}\})$ which is an open subset of $C_1 \times C_2$ and thus inherits the quasi-Hamiltonian structure (recall that a regular elliptic element is one whose angles are distinct and non-zero, see [G] p. 203).

We will analyze in more detail the differential properties of this map in sections 2.4 and 2.5.

2.3 Walls and reducible groups

In this section we describe in detail the collection W_{red} of reducible walls. The two elliptic conjugacy classes C_1 and C_2 are given by two angle pairs $\{\theta_1, \theta_2\}$ and $\{\theta_3, \theta_4\}$ normalized so that $\theta_i \in [0; 2\pi[$. We will look at the image of $\tilde{\mu}$ in the affine chart $\{(\theta_5, \theta_6) | \, \theta_i \in [0; 2\pi[, \theta_5 \geqslant \theta_6\}$ of $\mathbb{T}^2/\mathfrak{S}_2$ (we will use unordered pairs as long as we don't know which coordinate is larger).

As we have said, W_{red} is a trivalent graph with two vertices $D_1 = \{\theta_1+\theta_3, \theta_2+\theta_4\}$ and $D_2 = \{\theta_2+\theta_3, \theta_1+\theta_4\}$; these vertices are joined by the segment U of spherical reducible groups which has slope -1. If the two vertices have same index as defined in [FW1] (this means that they are on the same antidiagonal line in the affine chart), then U is simply the line segment joining them. If they have distinct indices (meaning that they are on two parallel antidiagonal lines in the affine chart), then U is the segment (disconnected in the affine chart) joining them by going through the sides of the square. Note that in both cases U is the shortest geodesic segment joining the vertices.

Each vertex is also the endpoint of two segments of hyperbolic reducible groups which go to the boundary of the square (and may even sometimes wrap once around the torus, see below), one of slope 2 and the other of slope 1/2. We will label these segments C_{13} and C_{24} through D_1, and C_{23} and C_{14} through D_2 (the notation will become clear below).

2.3.1 Totally reducible groups: the two vertices

These two points are the angle pairs of the product AB when A and B are simultaneously in diagonal form. Write these as $A = Diag(e^{i\theta_1}, e^{i\theta_2}, 1)$ and $B = Diag(e^{i\theta_3}, e^{i\theta_4}, 1)$ and we obtain $D_1 = \{\theta_1 + \theta_3, \theta_2 + \theta_4\}$; using $B = Diag(e^{i\theta_4}, e^{i\theta_3}, 1)$, we obtain $D_2 = \{\theta_1 + \theta_4, \theta_2 + \theta_3\}$.

2.3.2 Groups fixing a point

The question of eigenvalues of the product of matrices with fixed conjugacy classes in $U(2)$ has been studied in [Bi1] from the point of view of holomorphic bundles over the projective line, and in [FMS] from the point of view of the geometry of Lagrangian triples in $\mathbb{C}^2$. We will begin by quoting from [FW1] the following description of the allowed region for these eigenvalues, which they obtain by following the Biswas' method.

Their notation is a bit different from ours because they consider representations in $U(2)$ of the fundamental group of the thrice-punctured sphere with presentation

$$\langle A, B, C \mid A.B.C = 1 \rangle$$

The conditions involve the notion of *index* I of a representation which is an integer; in the notation of [FW1], I is the sum of angles of all six eigenvalues of the generators, each normalized in $[0, 1[$. In the case of Lagrangian representations (see next section), this index is in one-to-one correpondence with the Maslov index (or inertia index) of the Lagrangian triple. In our notation, the index of the representation (given by A, B and $(AB)^{-1}$) is written:

$$I = 2 + \frac{1}{2\pi}(\theta_1 + \theta_2 + \theta_3 + \theta_4 - \theta_5 - \theta_6)$$

The result is then that the allowable region for the sextuples of angles is a union of convex polyhedra in parallel hyperplanes corresponding to admissible integer values of the index I. The explicit inequalities involve the following quantities:

- $MM := \mathrm{Max}\{\theta_1, \theta_2\} + \mathrm{Max}\{\theta_3, \theta_4\}$
- $mm := \min\{\theta_1, \theta_2\} + \min\{\theta_3, \theta_4\}$
- $Mm := \mathrm{Max}\{\min\{\theta_1, \theta_2\} + \mathrm{Max}\{\theta_3, \theta_4\}, \mathrm{Max}\{\theta_1, \theta_2\} + \min\{\theta_3, \theta_4\}\}$

Proposition 2.1 (see [Bi1], [FW1]) *Let $A, B \in U(2)$ with respective angles $\{\theta_1, \theta_2\}$ and $\{\theta_3, \theta_4\}$, with $\theta_i \in [0; 2\pi[$. Then the possible angle pairs for the product AB are (θ_5, θ_6) (with $\theta_i \in [0; 2\pi[$ and $\theta_5 \geqslant \theta_6$) satisfying one of the following conditions:*

- *$I = 2$ (i.e. $\theta_5 + \theta_6 = \theta_1 + \theta_2 + \theta_3 + \theta_4$) and:*

$$\begin{cases} \theta_5 & \geqslant & Mm \\ \theta_6 & \geqslant & mm \end{cases}$$

- *$I = 3$ (i.e. $\theta_5 + \theta_6 = \theta_1 + \theta_2 + \theta_3 + \theta_4 - 2\pi$) and:*

$$\begin{cases} \theta_5 & \geqslant & MM - 2\pi \\ \theta_6 & \geqslant & Mm - 2\pi \\ \theta_6 & \leqslant & MM - 2\pi \end{cases}$$

- *$I = 4$ (i.e. $\theta_5 + \theta_6 = \theta_1 + \theta_2 + \theta_3 + \theta_4 - 4\pi$) and:*

$$\begin{cases} \theta_5 & \geqslant & Mm - 2\pi \\ \theta_6 & \geqslant & mm - 2\pi \end{cases}$$

The geometric picture is not obvious from these inequalities; in fact, for fixed pairs $\{\theta_1, \theta_2\}$ and $\{\theta_3, \theta_4\}$, one of the three cases above is empty, if not two. We now translate this result in our setting. The image is then simply the convex segment joining the vertices D_1 and D_2, i.e. the shortest geodesic segment between them, see section 2.5. Note that this shortest segment is always included in a -1-sloped line of the torus, even when the segment is disconnected in the affine chart.

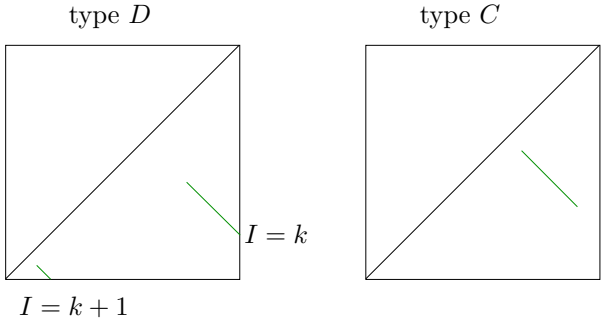

Figure 2: Configurations of spherical reducible groups

Proposition 2.2 *Let $A, B \in U(2)$ with respective angles $\{\theta_1, \theta_2\}$ and $\{\theta_3, \theta_4\}$, with $\theta_i \in \mathbb{R}/2\pi\mathbb{Z}$. Then the angles of the product AB are any pair $\{\theta_5, \theta_6\}$ lying in the convex segment of $\mathbb{T}^2/\mathfrak{S}_2$ joining the two totally reducible vertices $D_1 = \{\theta_1 + \theta_3, \theta_2 + \theta_4\}$ and $D_2 = \{\theta_2 + \theta_3, \theta_1 + \theta_4\}$.*

Concretely, in the affine chart $\{(\theta_5, \theta_6) | \, \theta_i \in [0; 2\pi[, \theta_5 \geqslant \theta_6\}$ of $\mathbb{T}^2/\mathfrak{S}_2$, this segment is:

- *the usual Euclidian segment (of slope -1) joining D_1 and D_2 if these two vertices have same index.*
- *the union of two Euclidian segments of slope -1, each going from a vertex to the horizontal or vertical boundary of the chart, if the vertices have different index .*

We will call such a configuration of *type C* (connected) in the first case, and of *type D* (disconnected) in the second case, see figure 2. Note that the fact that all these points lie on a common line of slope -1 of the torus simply expresses that the determinant of the product is the product of determinants.

2.3.3 Hyperbolic reducible groups

We now focus on the hyperbolic reducible groups, those which stabilize a $\mathbb{C}$-plane (or complex geodesic), that is a copy of $H^1_{\mathbb{C}}$ in $H^2_{\mathbb{C}}$. The decription simply comes from analyzing the product of matrices in block-diagonal form in $U(2,1)$, together with a characterization of the (oriented) angles of a triangle in the hyperbolic plane.

The totally reducible groups each stabilize two $\mathbb{C}$-planes intersecting at the common fixed point, so we expect that, by deformation, the corresponding vertex will be contained in two distinct hyperbolic reducible families. This is indeed the case, except in the degenerate cases when one generator (or both) is a $\mathbb{C}$-reflection (one angle is 0) or a complex reflection in a point (two equal angles). For instance, in matrix form, one hyperbolic reducible family containing the vertex D_1, which we will denote by C_{24}, is given by the following generators:

$$A = \begin{pmatrix} e^{i\theta_1} & 0 & 0 \\ 0 & e^{i\theta_2} & 0 \\ 0 & 0 & 1 \end{pmatrix} \quad \text{and} \quad B = \begin{pmatrix} e^{i\theta_3} & 0 & 0 \\ 0 & b_1 & b_2 \\ 0 & b_3 & b_4 \end{pmatrix}$$

where the conjugacy class of:

$$\widetilde{B} = \begin{pmatrix} b_1 & b_2 \\ b_3 & b_4 \end{pmatrix} \in U(1,1)$$

is given by its eigenvalues: $e^{i\theta_4}$ of positive type and 1 of negative type (this simply means that $\widetilde{B}$ acts on $H^1_{\mathbb{C}}$ by a rotation of θ_4). Recall that the type of an eigenvalue refers to the position of its associated eigenspace relative to the null cone of the Hermitian form (here, in $\mathbb{C}^{1,1}$). The other three hyperbolic reducible families C_{23}, C_{14}, and C_{13} are defined in the same way, exchanging the roles via $\theta_1 \leftrightarrow \theta_2$ and $\theta_3 \leftrightarrow \theta_4$.

In each family the product AB, as long as it is elliptic, has two angles θ_F and θ_N. We denote θ_C the angle of rotation in the stable $\mathbb{C}$-plane; θ_N is then the angle of rotation in the normal $\mathbb{C}$-planes. The result is then the following:

Proposition 2.3 *Let A, B be two elliptic elements in $PU(2,1)$ with respective angles $\{\theta_1, \theta_2\}$ and $\{\theta_3, \theta_4\}$ (with $\theta_i \in [0, 2\pi[$), such that the product AB is elliptic. If the group generated by A and B is hyperbolic reducible, then the angle pair $\{\theta_C, \theta_N\}$ of AB is in one of the four following segments:*

$$C_{24}: \begin{cases} \theta_C = 2\theta_N + \theta_2 + \theta_4 - 2\theta_1 - 2\theta_3 \ [2\pi] \quad and \\ \theta_2 + \theta_4 < \theta_C < 2\pi \quad (if \ \ \theta_2 + \theta_4 < 2\pi) \\ 0 < \theta_C < \theta_2 + \theta_4 - 2\pi \quad (if \ \ \theta_2 + \theta_4 > 2\pi). \end{cases}$$

$$C_{13}: \begin{cases} \theta_C = 2\theta_N + \theta_1 + \theta_3 - 2\theta_2 - 2\theta_4 \ [2\pi] \quad and \\ \theta_1 + \theta_3 < \theta_C < 2\pi \quad (if \ \ \theta_1 + \theta_3 < 2\pi) \\ 0 < \theta_C < \theta_1 + \theta_3 - 2\pi \quad (if \ \ \theta_1 + \theta_3 > 2\pi). \end{cases}$$

$$C_{23}: \begin{cases} \theta_C = 2\theta_N + \theta_2 + \theta_3 - 2\theta_1 - 2\theta_4 \ [2\pi] \quad and \\ \theta_2 + \theta_3 < \theta_C < 2\pi \quad (if \ \ \theta_2 + \theta_3 < 2\pi) \\ 0 < \theta_C < \theta_2 + \theta_3 - 2\pi \quad (if \ \ \theta_2 + \theta_3 > 2\pi). \end{cases}$$

$$C_{14}: \begin{cases} \theta_C = 2\theta_N + \theta_1 + \theta_4 - 2\theta_2 - 2\theta_3 \ [2\pi] \quad and \\ \theta_1 + \theta_4 < \theta_C < 2\pi \quad (if \ \ \theta_1 + \theta_4 < 2\pi) \\ 0 < \theta_C < \theta_1 + \theta_4 - 2\pi \quad (if \ \ \theta_1 + \theta_4 > 2\pi). \end{cases}$$

Note that each of these four segments has an endpoint which is a totally reducible vertex, the other endpoint being on one of the sides of the square; it is however possible that the segment wrap once around the torus before reaching its endpoint (see the examples section). We leave the inequalities in this form, which don't make apparent which segments have slope 2 and 1/2, because typically this can change inside the same family (in the case when the segment bounces off the diagonal of the square). For instance, if $\theta_1 + \theta_3 < \theta_2 + \theta_4 < 2\pi$, the segment C_{24} has slope 2 (at least, close to D_1) and C_{13} has slope 1/2 (also, close to D_1).

Proof. We treat the case of the family C_{24} whose generators are written above, A in diagonal form and B in block-diagonal form. Then the product $C = AB$ is also in block-diagonal form:

$$C = \begin{pmatrix} e^{i(\theta_1+\theta_3)} & 0 & 0 \\ 0 & c_1 & c_2 \\ 0 & c_3 & c_4 \end{pmatrix} \quad \text{with} \quad \widetilde{C} = \begin{pmatrix} c_1 & c_2 \\ c_3 & c_4 \end{pmatrix} \in U(1,1)$$

$\widetilde{C}$ has two eigenvalues of norm 1, say $e^{i\psi_1}$ and $e^{i\psi_2}$ with the latter of negative type. Then the angles of rotation of C are given by dividing the two eigenvalues of positive type by that of negative type. This is written:

$$\begin{cases} \theta_C = \psi_1 - \psi_2 \\ \theta_N = \theta_1 + \theta_3 - \psi_2 \end{cases}$$

Now we have again a condition coming from the determinant, which says here that $\psi_1 + \psi_2 = \theta_2 + \theta_4 \ [2\pi]$. Combining these equations, we obtain the condition: $\theta_C = 2\theta_N + \theta_2 + \theta_4 - 2\theta_1 - 2\theta_3 \ [2\pi]$.

The exact range of θ_C inside this line is given by the geometric condition which says what the possible third angle is for a triangle in the hyperbolic plane having two prescribed angles. The following lemma is just an oriented version of the fact that triangles exist in the hyperbolic plane if and only if their angle sum is less than π:

Lemma 2.1 *Let $\tilde{A}$ and $\tilde{B}$ be two elliptic isometries of $H^1_{\mathbb{C}}$, with respective rotation angles θ_2 and θ_4 ($\theta_i \in [0, 2\pi[$). As the fixed points of $\tilde{A}$ and $\tilde{B}$ vary, the rotation angle θ_C of the product $\tilde{C} = \tilde{A}\tilde{B}$ (when it is elliptic) ranges over the interval $[\theta_2 + \theta_4, 2\pi[$ if $\theta_2 + \theta_4 < 2\pi$, and $[0, \theta_2 + \theta_4 - 2\pi[$ if $\theta_2 + \theta_4 > 2\pi$.*

This completes the proof. □

2.3.4 Classifying the configurations of reducibles

We start by concentrating on the local configuration at each vertex. We have seen that the spherical reducible configurations are of two types, connected (type C) or disconnected (type D) in the half-square affine chart. As for the hyperbolic reducible configurations, we have just seen that two segments emanate from each vertex, one

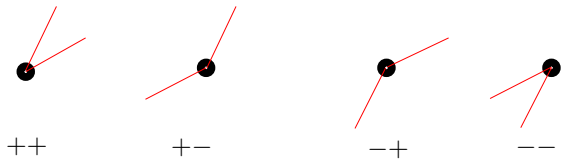

Figure 3: Local hyperbolic reducible types

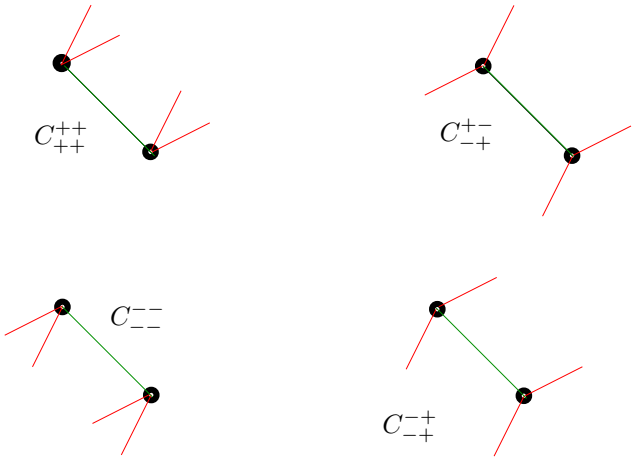

Figure 4: Local configurations of type C

of slope 2 and the other of slope 1/2. The direction of each segment, upward or downward from the vertex, is determined by the following data (see Prop. 2.3). We denote, for $i = 1, 2$ and $j = 3, 4$:

$$\sigma_{ij} := \theta_i + \theta_j$$

(where we have again normalized with $\theta_i \in [0, 2\pi[$). Then, at the vertex $\{\sigma_{ij}, \sigma_{kl}\}$ (see section 2.3.1), the segment C_{ij} goes upward if and only if $\sigma_{ij} < 2\pi$ (and C_{kl} goes upward if and only if $\sigma_{kl} < 2\pi$).

We will then assign a symbol to each configuration of reducibles, consisting in a letter (C or D) for the spherical reducible type and four $+$ or $-$ signs, arbitrarily ordered as follows. There are two pairs of signs, each corresponding to a vertex. The top pair corresponds to the "top" vertex (that with larger θ_6 in the affine chart $\{(\theta_5, \theta_6) | \, \theta_i \in [0; 2\pi[, \theta_5 \geqslant \theta_6\}$), and in each pair we have put the segment with slope 2 first. A $+$ sign means that the corresponding segment goes upward; see Figure 3 and examples in Figures 4 and 5. There are a priori 32 possibilities of such symbols, but in fact only 4 of type C and 4 of type D correspond to configurations of reducibles which actually occur. They are listed in the following result.

Proposition 2.4 *The possible local types of reducible configurations are, with the above notation,* C^{++}_{++}, C^{--}_{--}, C^{-+}_{-+}, C^{+-}_{-+} *and* D^{++}_{-+}, D^{++}_{+-}, D^{-+}_{--}, D^{+-}_{--} *(see Figures 4 and 5).*

Proof. We use three different criteria to discard the non-admissible configurations, then give examples of the remaining types. This is made easier by the fact that there is a symmetry among types which we will make explicit, after introducing some useful notation.

The hyperbolic reducible configurations are determined by the position of each $\sigma_{ij} = \theta_i + \theta_j$ (with $\theta_i \in [0, 2\pi[$ and $i = 1, 2$, $j = 3, 4$) relatively to 2π. This is nicely expressed in terms of the integer parts k_{ij} of $\frac{\sigma_{ij}}{2\pi}$, whose value is accordingly 0 or 1. These integers also appear when we normalize the cooordinates of the vertices in the affine chart, as we will see.

The symmetry is then as follows. Recall that each configuration is defined by the choice of two unordered pairs of angles, $\{\theta_1, \theta_2\}$ and $\{\theta_3, \theta_4\}$, with $\theta_i \in [0, 2\pi[$. The transformation S which we consider is simply taking each θ_i to its complementary (or symmetric) angle $2\pi - \theta_i$. This is interesting because obviously:

$$\theta_i + \theta_j < 2\pi \iff S(\theta_i) + S(\theta_j) > 2\pi$$

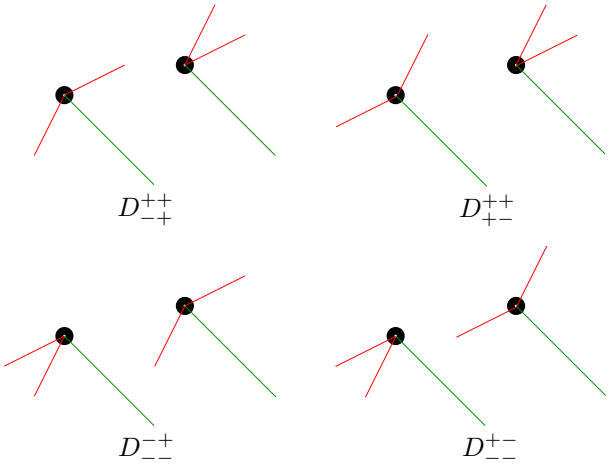

Figure 5: Local configurations of type D

(in other words: $S(k_{ij}) = 1 - k_{ij}$) so that all the signs of the hyperbolic reducible segments are exchanged. However we have to be a bit careful to see the effect on the whole configuration, because this also mixes up the vertices and their coordinates. First of all, the spherical reducible types C and D are stable under this transformation, because of the following characterization of type D (with as above $k_{ij} = Int(\frac{\sigma_{ij}}{2\pi})$):

Lemma 2.2 *The two vertices have a different index* $\iff$ $k_{13} + k_{24} \neq k_{14} + k_{23}$.

Proof of lemma. This follows simply by writing the indices in question. The only thing to note is that the vertices have coordinates σ_{ij}, appropriately normalized in $[0, 2\pi[$ as $\sigma_{ij} - 2\pi k_{ij}$. Then, denoting I_i the index of the vertex D_i, we have:

$$\begin{cases} 2\pi I_1 = \theta_1 + \theta_2 + \theta_3 + \theta_4 + (2\pi - (\sigma_{13} - 2\pi k_{13})) + (2\pi - (\sigma_{24} - 2\pi k_{24})) \\ 2\pi I_2 = \theta_1 + \theta_2 + \theta_3 + \theta_4 + (2\pi - (\sigma_{14} - 2\pi k_{14})) + (2\pi - (\sigma_{23} - 2\pi k_{23})) \end{cases}$$

so that:

$$I_2 - I_1 = k_{14} + k_{23} - (k_{13} + k_{24})$$

□

Now we note what happens to the vertices when we apply the transformation S. In type D, the two vertices have different indices and S sends the vertex with lower index to the vertex with higher index, so that the "top" and "bottom" vertices are exchanged by S. In type C, the two vertices have same index but for instance the "top" vertex is closer to the diagonal, and this remains unchanged by S so that the "top" and "bottom" vertices are not exchanged.

Last, at each vertex the two hyperbolic reducible segments are exchanged (because the larger coordinate of a vertex becomes the smaller one of its image) and, as we have said, the signs are changed. The following examples will be of particular interest to us:

$$\begin{array}{ll} S(C^{+-}_{++}) = C^{+-}_{--} & S(C^{+-}_{+-}) = C^{+-}_{+-} \\ S(D^{++}_{+-}) = D^{+-}_{--} & S(D^{-+}_{--}) = D^{++}_{-+} \\ S(D^{--}_{+-}) = D^{+-}_{++} & S(D^{--}_{-+}) = D^{-+}_{++} \end{array}$$

Now that we have reduced the number of cases (except for those which are unfortunately stable under S), we exclude the unwanted configurations. The first thing to notice is that $\sigma_{13} + \sigma_{24} = \sigma_{14} + \sigma_{23}$; this discards the four types C^{++}_{--}, C^{--}_{++}, D^{++}_{--} and D^{--}_{++}. The next criterion follows from the above lemma which characterizes type D, knowing that $k_{ij} = 1$ corresponds to a $+$ sign. Thus, in type C the sum of the two top signs must be equal to that of the bottom signs (where "adding signs" is meant like 0 and 1 with $0 \neq 2$), whereas in type D the sums must be different.

This gets rid of half of the cases; now, using the symmetry we have described, we are only left with the announced admissible types along with four ambiguous cases: C^{+-}_{+-} and C^{-+}_{+-} which are symmetric under S, D^{--}_{+-} (with its image D^{+-}_{++}), and D^{--}_{-+} (with its image D^{-+}_{++}).

The four latter, of type D, are easily discarded by the observation that in that type, the only vertex which can have a double $-$ sign is the vertex of larger index.

As for the last cases, suppose that we have a configuration of type C with a $+$ and a $-$ sign at each vertex. We can suppose by reordering that $\theta_1 > \theta_2, \theta_3$ and $\theta_3 > \theta_4$. The assumption on the signs says that we have one of the two situations:

$$\sigma_{13} > \sigma_{23} > 2\pi > \sigma_{14} > \sigma_{24}$$

$$\sigma_{13} > \sigma_{14} > 2\pi > \sigma_{23} > \sigma_{24}$$

We use the following lemma, which follows from reducing the σ_{ij} in $[0, 2\pi[$:

Lemma 2.3 *A vertex $\{\sigma_{ij}, \sigma_{kl}\}$ with $\sigma_{ij} > 2\pi > \sigma_{kl}$ is of type:*

- $(-,+)$ *if* $\sigma_{kl} > \sigma_{ij} - 2\pi$
- $(+,-)$ *if* $\sigma_{kl} < \sigma_{ij} - 2\pi$.

Now two σ_{ij} which share a subscript are certainly in the first case (because $\sigma_{ij} - \sigma_{jk} = \theta_i - \theta_k$), so that a $(+,-)$ couple cannot occur twice in any of the two above situations. This discards type C^{+-}_{+-}. As for type C^{-+}_{+-}, if we have one vertex of type $(-,+)$ and one of type $(+,-)$, the lemma implies that the top vertex must be of type $(+,-)$ (indeed the top vertice is the one with the smaller difference of coordinates).

We finish the proof by giving examples of the remaining possible cases (see the last chapter of [P] for details). We give here only the corresponding values of the pairs $\{\theta_1, \theta_2\}$ and $\{\theta_3, \theta_4\}$.

The configuration for $\{\frac{2\pi}{3}, \frac{2\pi}{4}\}$,$\{\frac{2\pi}{5}, \frac{2\pi}{6}\}$ is of type C^{++}_{++}, and its image under S is of type C^{--}_{--}. The configuration for $\{\frac{2\pi}{3}, -\frac{2\pi}{4}\}$,$\{\frac{2\pi}{5}, -\frac{2\pi}{6}\}$ is of type C^{+-}_{-+} (stable under S). Type C^{-+}_{-+} (stable under S) is obtained for instance with pairs $\{2\pi - \varepsilon, \varepsilon\}$,$\{2\varepsilon, 3\varepsilon\}$, provided that $5\varepsilon < 2\pi$.

As for types D: D^{-+}_{--} is obtained with $\{\frac{2\pi}{4}, \frac{2\pi}{6}\}$, $\{-\frac{2\pi}{5}, -\frac{2\pi}{7}\}$ and its image under S is D^{++}_{-+}. Finally, type D^{+-}_{--} is obtained with $\{\frac{2\pi}{4}, -\frac{2\pi}{6}\}$, $\{\frac{2\pi}{5}, -\frac{2\pi}{7}\}$ and its image under S is D^{++}_{+-}. □

2.4 Chambers and irreducible groups

In this section we focus on the claim that pairs (A, B) such that the group generated by A and B is irreducible are sent to interior points of the image. This follows from the fact that the map $\tilde{\mu}$ is a submersion at such a point; in order to ensure that the source is a manifold (and identify its tangent space) we consider $\tilde{\mu}$ restricted to those elements whose product is regular elliptic (in the half-square affine chart, this means that we consider only the interior points of the triangle):

$$\tilde{\mu}_r : \left\{ \begin{array}{ccccc} (C_1 \times C_2) \cap \mu^{-1}(\{\text{regular elliptics}\}) & \stackrel{\mu}{\longrightarrow} & G & \stackrel{\pi}{\longrightarrow} & \mathbb{T}^2/\mathfrak{S}_2 \\ (A, B) & \longmapsto & AB & \longmapsto & \text{Angles}(AB) \end{array} \right.$$

Since the regular elliptic elements of $G = PU(2,1)$ form an open set (see [G] p. 203), the source is now an open subset of $C_1 \times C_2$ and thus is a manifold with the same tangent space. Before going into the details, we give the result:

Proposition 2.5 *Let $(A, B) \in C_1 \times C_2$ such that AB is regular elliptic and the group generated by A and B is irreducible. Then the differential of $\tilde{\mu}_r$ at (A, B) is surjective and thus $\tilde{\mu}_r$ is locally surjective at that point.*

This phenomenon was brought to our attention by the analog in the compact group $U(n)$, described in [FW1] (see lemma 2.4 below). Thus $\tilde{\mu}$ is of rank 2 at an irreducible; we will see in the next section that it is of rank 1 at a generic reducible, and of rank 0 at a totally reducible.

Note also that we prove a stronger version of this statement in section 3.1.1, using only a certain class of Lagrangian deformations.

Proof. We will consider separately the product map μ and the projection π from G to its conjugacy classes, showing that each is a submersion at an irreducible. We begin by recalling a few facts about the Lie group structure of $G = PU(2,1)$ and its conjugacy classes. Consider a conjugacy class with a preferred representative A (in our case, the conjugacy class being elliptic, we can choose A to be a diagonal matrix):

$$C_1 = \{P.A.P^{-1} \mid P \in PU(2,1)\}$$

This is a submanifold of G of dimension $dim(PU(2,1)) - dim(Z(A))$ where the centralizer $Z(A)$ is of dimension 2 if A is regular elliptic (as can be seen on the diagonal form with 3 distinct eigenvalues) and of dimension 4 if A has two equal eigenvalues. Recall that $PU(2,1)$ has dimension 8; we thus obtain dimension 6 for the regular elliptic classes, and 4 for the special elliptic classes (note that in all cases the submanifold consisting of Lagrangian decompositions has half of this dimension, see section 3). The tangent space to this conjugacy class at A is then:

$$T_A C_1 = \{XA - AX \mid X \in \mathfrak{g}\} = \{(X - AXA^{-1})A \mid X \in \mathfrak{g}\}$$

the latter expression identifying this subspace of $T_A G$ to the subspace $Im(Id - Ad_A)$ of $\mathfrak{g} = T_1 G$ by right translation by A^{-1} (or right Maurer-Cartan form). This is the point of view taken in [FW1], where the following result is derived, denoting by $\mathfrak{z}(A,B)$ the Lie algebra of the centralizer of the group generated by A and B (and taking the orthogonal subspace with respect to the Killing form):

Lemma 2.4 $Im(d_{(A,B)}\mu) = \mathfrak{z}(A,B)^{\perp}.AB$.

In the notation of [FW1], our μ is $\pi^{(1)}$; this result can be found in the proof of Prop. 4.2 on p. 23. We include a short proof for the reader's convenience. Write, for $h_1 \in T_A C_1$ and $h_2 \in T_B C_2$: $\mu(A + h_1, B + h_2) = AB + Ah_2 + h_1 B + h_1 h_2$. This gives the expression of the differential of μ at (A,B): $d_{(A,B)}\mu(h_1,h_2) = Ah_2 + h_1 B$. If we translate as before these tangent vectors into $\mathfrak{g} = T_1 G$ by writing $h_1 = X_1.A$, $h_2 = X_2.B$ (with $X_1 \in Im(Id - Ad_A)$ and $X_2 \in Im(Id - Ad_B)$) and $d_{(A,B)}\mu(h_1,h_2) = X_3.AB$, we obtain the cocycle relation:

$$X_3 = X_1 + Ad_A(X_2)$$

Using an Ad-invariant non-degenerate bilinear form on $\mathfrak{g}$ such as the Killing form, the lemma follows by noting that:

$$[Im(Id - Ad_A) + Ad_A(Im(Id - Ad_B)]^{\perp} = Ker(Id - Ad_A) \cap Ad_A(Ker(Id - Ad_B)) = \mathfrak{z}(A) \cap \mathfrak{z}(B)$$

Now if A and B generate an irreducible group, then $\mathfrak{z}(A,B) = \{0\}$ (because $PU(2,1)$ has trivial center), so that μ is indeed a submersion at such a point.

Finally, the projection π restricted to elliptic elements is in coordinates the map which to a matrix associates its eigenvalues (rather, two linear combinations of its eigenvalues), so that it is classically differentiable and a submersion at those points which yield distinct eigenvalues: these are the regular elliptic elements. □

2.5 Which chambers are full ?

It follows from the previous section that a chamber is either entirely in the image of $\tilde{\mu}$ ("full") or entirely in its complement ("empty"). We have two types of arguments to determine which chambers are full and which are empty: constructive arguments such as local convexity tell us that some chambers must be full, and obstructions which force other chambers to be empty.

There is a natural notion of convexity in the surface $\mathbb{T}^2/\mathfrak{S}_2$ as in any Riemannian manifold (or orbifold), that of geodesic convexity. The only subtlety arises from the fact that there are (as in the torus) many geodesic segments joining two points, and sometimes there is not a unique shortest path among them. However, such pairs of points are isolated so we don't really need to worry about them in the definition of convexity.

Definition 2.1 *A subset C of $\mathbb{T}^2/\mathfrak{S}_2$ will be called* **convex** *if for all pairs of points $(x,y) \in C^2$ which are joined by a unique shortest geodesic segment, this segment is contained in C.*

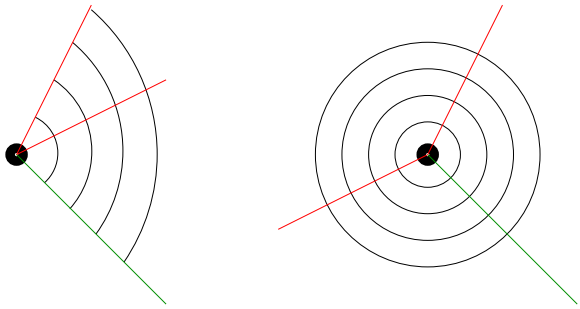

Figure 6: Local convexity around a totally reducible vertex

In fact we only need here the notion of local convexity in the neighborhood of a vertex; this notion is clear because the surface $\mathbb{T}^2/\mathfrak{S}_2$ has an affine structure (as a quotient of $\mathbb{R}^2$ by a group of affine transformations). There are two types of vertices which appear in the present case: the two totally reducible vertices which we have already seen and some "accidental" vertices which occur when two hyperbolic reducible families meet (of course only their images meet). The local structure around the totally reducible vertices is of fundamental importance and we conjecture that it determines the whole image; as for the accidental vertices, the two polygons arising from distinct regions of the source seem to overlap without interfering. Our main argument of local convexity at a totally reducible vertex relies on the differential properties of $\tilde{\mu}$ at such a point; namely we show that the first differential is null, but that **if one of A or B is not a complex reflection** the second differential is non-null along the reducible segments, so that the image is locally a convex cone bounded by the reducible walls. The main result is the following:

Proposition 2.6 *If one of A or B is not a complex reflection, then the image of $\tilde{\mu}$ contains all chambers which touch a totally reducible vertex and meet the local convex hull of the three reducible walls containing that vertex. In particular, if these three walls meet with obtuse angles, then the vertex is an interior point of the image (see Figure 6).*

Proof. We begin with the following lemma which completes what we have seen before, namely that $\tilde{\mu}$ is of rank 2 at an irreducible:

Lemma 2.5

- *If A and B generate a totally reducible group, then $d_{(A,B)}\tilde{\mu}$ is null.*
- *If A and B generate a generic reducible group (i.e. whose image is an interior point of a wall), then $d_{(A,B)}\tilde{\mu}$ is of rank 1.*

Proof of lemma. We have seen during the study of irreducible points (lemma 2.4) that :

$$Im(d_{(A,B)}\mu) = \mathfrak{z}(A,B)^{\perp}.AB$$

We have also seen that the centralizer of a regular elliptic element is of dimension 2 (that of a special elliptic being 4), so that if A or B is regular elliptic, the dimension of $\mathfrak{z}(A,B)$ is 2 for a totally reducible group and 1 for a generic reducible group. It only remains to see that the subspace $Im(d_{(A,B)}\mu)$ is tangent to the fiber of π at a totally reducible (respectively contains the tangent space of the fiber at a generic reducible). But this is clear because $Im(d_{(A,B)}\mu) = \mathfrak{z}(A,B)^{\perp}.AB$ always contains the tangent space to the fiber which is $T_{AB}C_3 = \mathfrak{z}(AB)^{\perp}.AB$ (where C_3 denotes the conjugacy class of AB). □

We then focus on a totally reducible vertex where the image will be locally described by the second differential.

Lemma 2.6 *The image of the quadratic differential $Q : v \longmapsto d^2_{(A,B)}\tilde{\mu}(v,v)$ is a convex cone in $\mathbb{R}^2$.*

Proof of lemma. This is a general fact about quadratic maps; we include a short proof in the case where the image is of dimension 2. Denote $B(v,w) = d^2_{(A,B)}\tilde{\mu}(v,w)$ the associated symmetric bilinear map and

$Q(v) = B(v,v)$. The image of Q is clearly a cone (because $Q(\lambda v) = \lambda^2 Q(v)$ for $\lambda \in \mathbb{R}$). To show that it is convex, consider two vectors $w_1 = Q(v_1)$ and $w_2 = Q(v_2)$ in the image; we show that the whole segment $[w_1, w_2]$ is in the image of the plane spanned by v_1 and v_2. Indeed, suppose that w_1 and w_2 are linearly independant and write, for $\lambda, \mu \in \mathbb{R}$:

$$Q(\lambda v_1 + \mu v_2) = \lambda^2 w_1 + \mu^2 w_2 + 2\lambda\mu B(v_1, v_2) = (\lambda^2 + 2\lambda\mu x_1)w_1 + (\mu^2 + 2\lambda\mu x_2)w_2$$

where we have expressed $B(v_1, v_2) = x_1 w_1 + x_2 w_2$ in the basis (w_1, w_2). It suffices to prove that the ratio of the two coordinates $f(\lambda, \mu) = \frac{\mu^2 + 2\lambda\mu x_2}{\lambda^2 + 2\lambda\mu x_1}$ surjects $\mathbb{R}^+$. But this is clear because the map f is continuous outside of the two lines $\{\lambda = 0\}, \{\lambda + 2\mu x_1 = 0\}$ and for instance on a line $\{\mu = p\lambda\}$ it takes the value $\frac{p^2 + 2px_2}{1 + 2px_1}$ which takes all values between 0 and $+\infty$ (in two of the four quadrants where f is defined). □

It remains to find non-null vectors in the image of Q tangent to the reducible segments.

Lemma 2.7
- *If neither A nor B is a complex reflection in a point (i.e. if $\theta_1 \neq \theta_2$ and $\theta_3 \neq \theta_4$), then at each totally reducible vertex the spherical reducible family contains paths with a non-null second derivative.*
- *If neither A nor B is a complex reflection (i.e. if $\theta_i \neq 0$ for $i = 1...4$) then at its totally reducible vertex each hyperbolic reducible family contains paths with a non-null second derivative.*

Proof of lemma. We show this by an explicit computation of deformations in the neighborhood of a totally reducible vertex, along the Lie algebra of $U(2)$ on one hand and of $U(1,1)$ on the other. In fact, we compute the second derivative not of the map $\tilde{\mu}$ itself (the angle pair) but of the trace of the product matrix, which is equivalent (at least locally, see chapter 1) and simplifies the computation greatly. Note that we don't normalize the determinant of the product matrix, but this doesn't matter because it only depends on $\theta_1, \theta_2, \theta_3, \theta_4$ so it is invariant by deformation.

We thus consider A and B in diagonal form (a totally reducible point) and write deformations of B inside its conjugacy class as a path $h(t).B.h(t)^{-1}$ where $h(t)$ is a path in $U(2,1)$ with $h(0) = 1$. We will then specialize to the cases where $\dot{h}(0)$ is in $\mathfrak{u}(2)$ or $\mathfrak{u}(1,1)$ (with the notation $\dot{h} = \frac{dh}{dt}$). We begin by computing the second derivative, noting that $\frac{d(h^{-1})}{dt} = -h^{-1}\dot{h}h^{-1}$:

$$\begin{aligned}
\tfrac{d^2}{dt^2} Tr(A.hBh^{-1})(0) &= \tfrac{d}{dt} Tr(A\dot{h}Bh^{-1} - AhBh^{-1}\dot{h}h^{-1})(0) \\
&= Tr(A\ddot{h}B - 2A\dot{h}B\dot{h} - AB(-\dot{h})\dot{h} - AB\ddot{h} - AB\dot{h}(-\dot{h}))(0) \\
&= 2Tr(AB\dot{h}^2 - A\dot{h}B\dot{h})(0)
\end{aligned}$$

where we have simplified repeatedly by $h(0) = h^{-1}(0) = 1$ and used the fact that A and B commute. We compute this last expression for $\dot{h}(0) \in \mathfrak{u}(2)$ then $\mathfrak{u}(1,1)$. Recall that:

$$U(2) = \{A \in GL(2,\mathbb{C}) \mid A.A^* = 1\} \text{ so that}$$

$$\mathfrak{u}(2) = \{A \in M(2,\mathbb{C}) \mid A + A^* = 0\} = \left\{ \begin{pmatrix} ri & b \\ -\overline{b} & si \end{pmatrix} \mid r, s \in \mathbb{R},\ b \in \mathbb{C} \right\}$$

With this latter expression for $\dot{h}$, writing A and B as diagonal matrices in $U(2)$ (here $A = Diag(e^{i\theta_1}, e^{i\theta_2})$ and $B = Diag(e^{i\theta_3}, e^{i\theta_4})$), we obtain:

$$AB\dot{h}(0)^2 = \begin{pmatrix} -(r^2 + |b|^2)e^{i(\theta_1+\theta_3)} & (r+s)ibe^{i(\theta_1+\theta_3)} \\ -(r+s)i\overline{b}e^{i(\theta_2+\theta_4)} & -(s^2+|b|^2)e^{i(\theta_2+\theta_4)} \end{pmatrix}$$

$$A\dot{h}(0)B\dot{h}(0) = \begin{pmatrix} -r^2e^{i(\theta_1+\theta_3)} - |b|^2e^{i(\theta_1+\theta_4)} & bi(re^{i(\theta_1+\theta_3)} + se^{i(\theta_1+\theta_4)}) \\ -\overline{b}i(re^{i(\theta_2+\theta_3)} + se^{i(\theta_2+\theta_4)}) & -s^2e^{i(\theta_2+\theta_4)} - |b|^2e^{i(\theta_2+\theta_3)} \end{pmatrix}$$

so that:

$$Tr(AB\dot{h}^2 - A\dot{h}B\dot{h})(0) = |b|^2(e^{i(\theta_1+\theta_4)} + e^{i(\theta_2+\theta_3)} - e^{i(\theta_1+\theta_3)} - e^{i(\theta_2+\theta_4)})$$

This gives us the result for $U(2)$ because this complex number, sum of four terms of equal norm, is non-zero as long as ($b \neq 0$ and) the terms are not pairwise equal (as in a rhombus), that is if $\theta_1 \neq \theta_2$ and $\theta_3 \neq \theta_4$. Note that the second derivative is always in the same half-line of the complex plane.

Now we do the same thing for $\dot{h}(0) \in \mathfrak{u}(1,1)$. Recall that, denoting $J = Diag(1,-1)$:

$$U(1,1) = \{A \in GL(2,\mathbb{C}) \mid A.J.A^* = J\} \text{ so that}$$

$$\mathfrak{u}(1,1) = \{A \in M(2,\mathbb{C}) \mid AJ + JA^* = 0\} = \left\{ \begin{pmatrix} ri & b \\ \overline{b} & si \end{pmatrix} \mid r,s \in \mathbb{R},\ b \in \mathbb{C} \right\}$$

We use this latter expression for $\dot{h}(0)$, and write only the block of A and B corresponding to the stable $\mathbb{C}$-plane as a diagonal matrix in $U(1,1)$ (for instance, $A = Diag(e^{i\theta_2}, 1)$ and $B = Diag(e^{i\theta_4}, 1)$ correspond to the family C_{24} of Prop. 2.3). We obtain:

$$AB\dot{h}(0)^2 = \begin{pmatrix} (|b|^2 - r^2)e^{i(\theta_2+\theta_4)} & (r+s)ibe^{i(\theta_2+\theta_4)} \\ (r+s)i\overline{b} & |b|^2 - s^2 \end{pmatrix}$$

$$A\dot{h}(0)B\dot{h}(0) = \begin{pmatrix} -r^2e^{i(\theta_2+\theta_4)} + |b|^2e^{i\theta_2} & bi(re^{i(\theta_2+\theta_4)} + se^{i\theta_2}) \\ \overline{b}i(re^{i\theta_4} + s) & |b|^2e^{i\theta_4} - s^2 \end{pmatrix}$$

so that:

$$Tr(AB\dot{h}^2 - A\dot{h}B\dot{h})(0) = |b|^2(e^{i(\theta_2+\theta_4)} + 1 - e^{i\theta_2} - e^{i\theta_4}).$$

As above, this number is non-zero for ($b \neq 0$ and) $\theta_2 \neq 0$ and $\theta_4 \neq 0$. We obtain the analogous condition for the three other hyperbolic reducible segments. □

This completes the proof of the proposition, except maybe for the cases where one of A or B is a complex reflection (resp. complex reflection in a point), and where A and B are complex reflections in a point, which the preceding lemma excluded. But this is only normal, because in each case the vanishing second derivative corresponds to a reducible family which is in fact reduced to a point. Precisely, if one of the generators has two equal angles then the two reducible vertices are equal and the spherical reducible segment is reduced to this point; if one of the angles is zero then the two corresponding hyperbolic reducible families collapse to a point (for instance, if $\theta_1 = 0$ then C_{13} and C_{14} collapse). □

2.6 Which chambers are empty?

We now describe various obstructions for certain chambers. We investigate in particular when the image of $\tilde{\mu}$ contains the three corners of the half-square affine chart, and determine which part of the diagonal is in the image. This allows us to prove theorem 1.2.

The main idea is to restore the original symmetry of the problem, by considering simultaneously the three generators A, B and C which satisfy $ABC = 1$. We then choose the most convenient pair among these (for the problem at hand), and consider the associated momentum map. As we will be considering different maps $\tilde{\mu}$ in this section, we will keep track of the generators by writing $\tilde{\mu}_{\{\theta_1,\theta_2\},\{\theta_3,\theta_4\}}$ instead of just $\tilde{\mu}$. We normalize $\{\theta_1,\theta_2\}, \{\theta_3,\theta_4\}$ so that $\theta_i \in [0, 2\pi[$ and $\theta_1 \geqslant \theta_2$, $\theta_3 \geqslant \theta_4$.

In the present case, we investigate when the diagonal corners of the half-square affine chart are in the image, so that one of these generators has angle pair $\{\varepsilon,\varepsilon\}$ or $\{2\pi-\varepsilon, 2\pi-\varepsilon\}$ for small ε. We use the fact that the image polygon is easily determined if one of the generators is of this type; we will thus change generators as described in the following lemma, which is obvious from the definitions:

Lemma 2.8

$$\{\varepsilon,\varepsilon\} \in \text{Im } \tilde{\mu}_{\{\theta_1,\theta_2\},\{\theta_3,\theta_4\}} \Longleftrightarrow \{\theta_3,\theta_4\} \in \text{Im } \tilde{\mu}_{\{2\pi-\theta_1,2\pi-\theta_2\},\{\varepsilon,\varepsilon\}}$$

Since $\{\theta_1,\theta_2\}$ remains fixed throughout the section, we will write $P_{\{\varepsilon,\varepsilon\}}$ for Im $\tilde{\mu}_{\{2\pi-\theta_1,2\pi-\theta_2\},\{\varepsilon,\varepsilon\}}$ (and $P_{\{-\varepsilon,-\varepsilon\}}$ for Im $\tilde{\mu}_{\{2\pi-\theta_1,2\pi-\theta_2\},\{2\pi-\varepsilon,2\pi-\varepsilon\}}$).

These two polygons are easily determined, using the fact that they can't contain points on the diagonal which are irreducible (this is a special case of proposition 4.1 below). Their description follows once we have determined the reducible walls. When one of the generators is a complex reflection in a point (i.e. has two equal angles), the wall structure degenerates: there is only one totally reducible vertex which is the endpoint of two

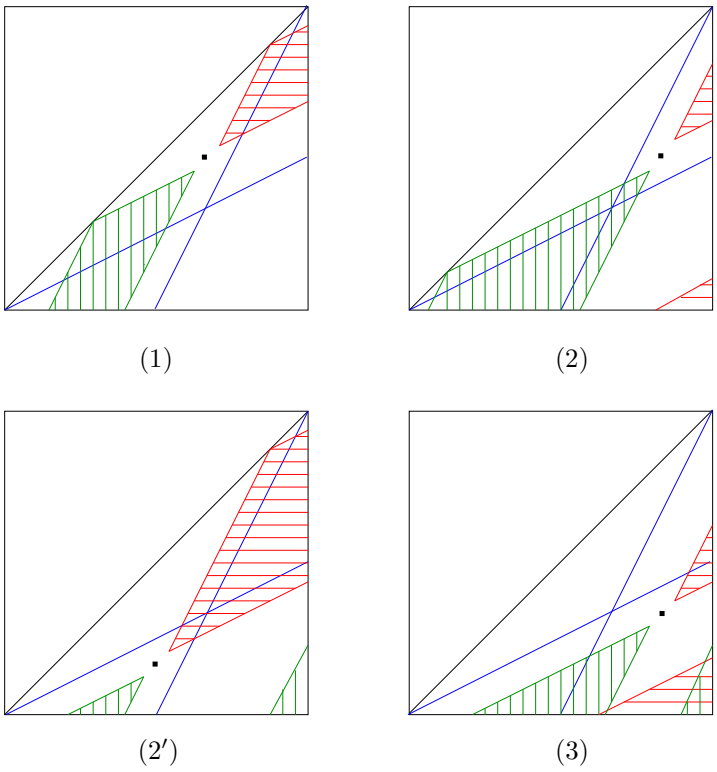

Figure 7: Auxiliary polygons for the two diagonal corners: the bold point is $(2\pi-\theta_2, 2\pi-\theta_1)$, $P_{\{\varepsilon,\varepsilon\}}$ has horizontal hatching, and $P_{\{-\varepsilon,-\varepsilon\}}$ has vertical hatching

hyperbolic reducible segments. We determine these from proposition 2.3; with pairs $\{\varepsilon,\varepsilon\}$ or $\{2\pi-\varepsilon, 2\pi-\varepsilon\}$ with small ε, the two relevant σ_{ij} are either both smaller than 2π or both greater. This means that the corresponding hyperbolic reducible segments both go upward (for $\{\varepsilon,\varepsilon\}$) or both downward (for $\{2\pi-\varepsilon, 2\pi-\varepsilon\}$). The possible types (by maybe allowing to diminish ε) only vary with the position of the vertex $(2\pi-\theta_2, 2\pi-\theta_1)$ (which is the limit vertex for $\varepsilon \to 0$) relative to the two lines $\{\theta_1 = 2\theta_2\}$ and $\{2(\theta_1 - 2\pi) = \theta_2 - 2\pi\}$.

We have illustrated the four possibilities in Figure 7, where both images $P_{\{\varepsilon,\varepsilon\}}$ and $P_{\{-\varepsilon,-\varepsilon\}}$ are drawn in each case. This immediately allows us to infer when both corners are in the image of $\tilde{\mu}_{\{\theta_1,\theta_2\},\{\theta_3,\theta_4\}}$. By the above lemma, this means that $P_{\{\varepsilon,\varepsilon\}}$ and $P_{\{-\varepsilon,-\varepsilon\}}$ overlap for ε small enough, and that the point (θ_3,θ_4) is in the intersection for all smaller ε. Note that this overlapping can happen in case (3) as in figure 7, but also in cases (2) and (2′) (which are symmetric), if the point $(2\pi-\theta_2, 2\pi-\theta_1)$ moves towards the boundary of the square. We write the equations of the lines corresponding to the reducible walls, and examine when they intersect. When this is the case, we write under which conditions the point (θ_3,θ_4) is in the intersection region. This is elementary and we leave the details to the reader. We obtain the following conditions:

$$(*)\begin{cases} 2\theta_1 - \theta_2 + 2\theta_3 - \theta_4 \geqslant 6\pi \\ \theta_1 - 2\theta_2 + \theta_3 - 2\theta_4 \geqslant 2\pi \end{cases}$$

which says that the point $(2\pi-\theta_2, 2\pi-\theta_1)$ is in case (3) and the point (θ_3,θ_4) is in the overlapping region. For case (2) we obtain:

$$(**)\begin{cases} 2\theta_2 - \theta_1 + 2\theta_3 - \theta_4 \leqslant 2\pi \\ 2\theta_2 - \theta_1 + 2\theta_4 - \theta_3 \leqslant -2\pi \end{cases}$$

and the conditions $(**')$ in case (2′) are obtained from the inequalities $(**)$ by sending each θ_i to $2\pi-\theta_i$ (which corresponds to the previous S, reflection along the antidiagonal). We have thus proven:

Proposition 2.7 *Let $\theta_1, ..., \theta_4 \in [0, 2\pi[$ with $\theta_1 \geqslant \theta_2$, $\theta_3 \geqslant \theta_4$. Then* Im $\tilde{\mu}_{\{\theta_1,\theta_2\},\{\theta_3,\theta_4\}}$ *contains pairs $\{\varepsilon,\varepsilon\}$ and $\{2\pi-\varepsilon, 2\pi-\varepsilon\}$ for ε arbitrarily small if and only if $\theta_1,\theta_2,\theta_3,\theta_4$ satisfy conditions $(*)$, $(**)$ or $(**')$.*

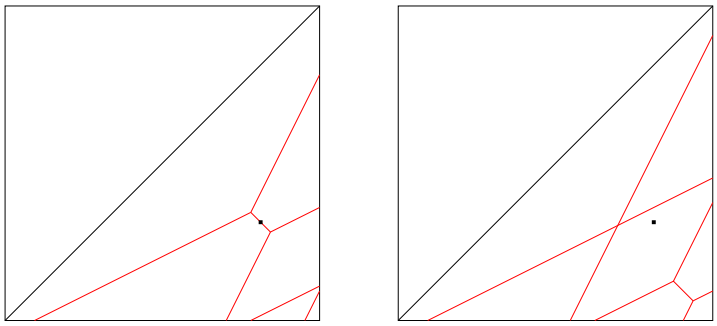

$P_{\{\varepsilon,-\varepsilon\}}$ Im $\tilde{\mu}_{\{\varepsilon,-\varepsilon\},\{\eta,-\eta\}}$

Figure 8: Auxiliary polygons (reducible framework) for the lower right corner: the bold point is $(2\pi-\theta_2, 2\pi-\theta_1)$

We then note that in cases $(**)$ (and $(**')$) Im $\tilde{\mu}_{\{\theta_1,\theta_2\},\{\theta_3,\theta_4\}}$ does not contain a internal portion of the diagonal. This follows from our decription, by varying the above pair $\{\varepsilon,\varepsilon\}$ for arbitrary ε (in the picture, this means moving the vertex of the polygon along a diagonal line).

It turns out that the third corner of the half-square (pairs $\{2\pi-\varepsilon,\varepsilon\}$ for ε arbitrarily small) is also in the image when condition $(*)$ is satisfied. In fact we prove the following stronger statement:

Proposition 2.8 *When $\theta_1,\theta_2,\theta_3,\theta_4$ satisfy condition $(*)$, $\tilde{\mu}_{\{\theta_1,\theta_2\},\{\theta_3,\theta_4\}}$ is onto.*

This will follow from the constructive arguments of the previous section (namely local convexity around the totally reducible vertices), once we have shown that the image contains the third corner, because we will also note that the reducible walls have the local structure C^{+-}_{-+} (see section 2.3.4). We prove these two facts before showing why they suffice.

Lemma 2.9 *If $\theta_1,\theta_2,\theta_3,\theta_4$ satisfy condition $(*)$ then* Im $\tilde{\mu}_{\{\theta_1,\theta_2\},\{\theta_3,\theta_4\}}$ *contains pairs $\{2\pi-\varepsilon,\varepsilon\}$ for ε arbitrarily small.*

Proof. We begin as above by changing generators; the change we use reads in terms of angle pairs as the following fact (see lemma 2.8):

$$\{2\pi-\varepsilon,\varepsilon\}\in \text{Im }\tilde{\mu}_{\{\theta_1,\theta_2\},\{\theta_3,\theta_4\}} \Longleftrightarrow \{\theta_3,\theta_4\}\in \text{Im }\tilde{\mu}_{\{2\pi-\theta_1,2\pi-\theta_2\},\{2\pi-\varepsilon,\varepsilon\}}$$

We will denote as before Im $\tilde{\mu}_{\{2\pi-\theta_1,2\pi-\theta_2\},\{2\pi-\varepsilon,\varepsilon\}}$ by $P_{\{\varepsilon,-\varepsilon\}}$. We are only concerned with the reducible walls of this image, which are given by the results of section 2.3. These walls are depicted in the first part of figure 8 (note that the local structure is of type C^{+-}_{-+} for ε small enough). If we denote by W_∞ the limit of this reducible structure as ε tends to 0, the key observation is that the reducible structure of $P_{\{\varepsilon,\varepsilon\}}\cup P_{\{-\varepsilon,-\varepsilon\}}$ degenerates to this same W_∞ as ε tends to 0. In other words, for ε tending to 0, the walls of $P_{\{\varepsilon,-\varepsilon\}}$ and $P_{\{\varepsilon,\varepsilon\}}\cup P_{\{-\varepsilon,-\varepsilon\}}$ determine the same chambers. By assumption, the point $\{\theta_3,\theta_4\}$ is in the lower right chamber of $P_{\{\varepsilon,\varepsilon\}}$ and $P_{\{-\varepsilon,-\varepsilon\}}$ for ε small enough (this is the geometric meaning of condition $(*)$). Thus the lemma is proven as soon as we know that $P_{\{\varepsilon,-\varepsilon\}}$ contains the lower right corner (pairs $\{2\pi-\eta,\eta\}$ for arbitrarily small η). We see this again by appropriately changing our generators, noting that:

$$\{2\pi-\eta,\eta\}\in \text{Im }\tilde{\mu}_{\{2\pi-\theta_1,2\pi-\theta_2\},\{2\pi-\varepsilon,\varepsilon\}} \Longleftrightarrow \{2\pi-\theta_1,2\pi-\theta_2\}\in \text{Im }\tilde{\mu}_{\{2\pi-\eta,\eta\},\{2\pi-\varepsilon,\varepsilon\}}$$

Now the latter image polygon has a simple reducible wall structure (which is depicted in the second part of figure 8 for small ε and η), from which one infers that the point $\{2\pi-\theta_1,2\pi-\theta_2\}$ (which, again by assumption, is in case (3) above) is in a chamber adjacent to a totally reducible vertex with obtuse wall angles. We conclude by proposition 2.6 that the point $\{2\pi-\theta_1,2\pi-\theta_2\}$ is in Im $\tilde{\mu}_{\{2\pi-\eta,\eta\},\{2\pi-\varepsilon,\varepsilon\}}$ for small ε and η. □

Lemma 2.10 *When $\theta_1,\theta_2,\theta_3,\theta_4$ satisfy condition $(*)$, the reducible walls have the local structure C^{+-}_{-+}.*

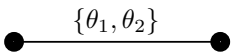

Figure 9: Coxeter diagram for a pair of $\mathbb{R}$-reflections

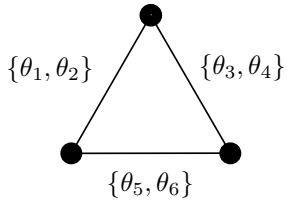

Figure 10: Coxeter diagram for a triple of $\mathbb{R}$-reflections

Proof. Adding the two inequalities of $(*)$, one obtains:

$$3(\theta_1 - \theta_2 + \theta_3 - \theta_4) \geqslant 8\pi$$

and in particular $\sigma_{13} - \sigma_{24} > 2\pi$ (recall that $\sigma_{ij} := \theta_i + \theta_j$). By lemma 2.3 the vertex $S_1 = \{\sigma_{13}, \sigma_{24}\}$ is then of type $(+,-)$. But the only type C configuration containing $(+,-)$ is C^{+-}_{-+}. □

3 Configurations of Lagrangian triples

We consider in this section a more restricted class of elliptic triangle groups, which we will call *Lagrangian* or *decomposable*. Namely these groups are of index 2 in a group generated by three $\mathbb{R}$-reflections (or antiholomorphic involutions) in $\mathbb{R}$-planes intersecting pairwise inside complex hyperbolic space. More pecisely, the two generators of the triangle group are products of two $\mathbb{R}$-reflections, one of these being common to both generators. This is analogous to the classical idea of considering (orientation-preserving) triangle groups of the plane (Euclidian, spherical, or hyperbolic) inside of a group generated by reflections in the sides of a triangle, which is how their geometric properties are usually analyzed.

Recall that an intersecting pair of Lagrangians is characterized up to isometry by a pair of (reflection) angles which are half of the (rotation) angles of the elliptic isometry obtained by composing the two associated $\mathbb{R}$-reflections. This produces an angle pair $\{\theta_1, \theta_2\}$ with $\theta_i \in \mathbb{R}/\pi\mathbb{Z}$, which we write in a Coxeter-type diagram (see figure 9). The question of the possible configurations of pairwise intersecting triples of $\mathbb{R}$-planes then translates into that of possible angle pairs as labels for the triangle graph of figure 10.

As in the classical case of planar groups, we gain some geometric information by introducing these $\mathbb{R}$-reflections; in fact we obtain a geometric obstruction which is completely analogous to the planar case in the sense that it expresses the admissible Riemannian angles in a geodesic triangle (see section 3.2). However, we have not found a way to express this condition on the three angle pairs in an elliptic triangle group which is not Lagrangian, although we conjecture that the image polygon must be the same (which in the case of the compact group $U(n)$ is the main theorem of [FW1]).

Apart from this specific obstruction, everything we have done for elliptic triangle groups carries over to the Lagrangian setting: on one hand, the restricted momentum map is also of maximal rank at an irreducible, and on the other, the reducible groups are exactly the same in both cases. We gain a lot for practical reasons though, mostly from the smaller dimension count at the source: the dimension of $\mathbb{R}$-reflections decomposing a given elliptic conjugacy class is 3 (see the last chapter of [P] for an explicit parametrization), half of that of the conjugacy class itself. This fits in with Schaffhauser's description of the space of decomposable groups as a Lagrangian submanifold of the symplectic representation manifold of a surface group (that of the punctured sphere inside $U(n)$, see [Sf]). From the practical viewpoint, $\mathbb{R}$-reflections give us a way of paramatrizing a given conjugacy class tranversally to the fibers of our momentum map (with half as many parameters); most notable is the fact that we obtain (generic) fibers of dimension 1, which is the starting point of our search for discrete groups in this setting (see last section).

3.1 Lagrangian triples vs. elliptic triangles

We consider here the map $\tilde{\mu}_L$ which is the restriction of the map $\tilde{\mu}$ of the preceding section (taking a pair of elliptic elements (A, B) in fixed conjugacy classes to the angle pair of their product) to pairs (A, B) which are *simultaneously decomposable* (into $\mathbb{R}$-reflections). This means that there exist $\mathbb{R}$-reflections σ_1, σ_2 and σ_3 such that $A = \sigma_2\sigma_1$ and $B = \sigma_3\sigma_2$ (it corresponds to Lagrangian representations in the terms of [FW1] and [Sf]). The angles of the product $BA = \sigma_3\sigma_1$ are then (double of) those of the corresponding $\mathbb{R}$-planes L_1 and L_3, which shows that the problems of the image of the Lagrangian momentum map $\tilde{\mu}_L$ and of possible configurations of triples of $\mathbb{R}$-planes are equivalent.

It is obvious that the image of $\tilde{\mu}_L$ is contained in that of $\tilde{\mu}$; we conjecture that, as in the case of $U(n)$ investigated in [FW1], these images must be equal. Evidence in favor of this is provided by the fact that all our constructive arguments from the preceding section (local surjectivity at an irreducible, description of reducibles and local convexity) carry over to the case of decomposable groups (see also the experimental pictures in the last chapter of [P], which we have obtained by a parametrization of decomposable groups). However, the obstruction on Lagrangian configurations of section 3.2 does not seem to carry over to the general unitary case, but it is possible that the corresponding chambers be eliminated in that case for different reasons.

3.1.1 Irreducible groups project to interior points

We begin by showing that the submanifold of decomposable pairs in $C_1 \times C_2$ is tranverse to the fibers of the momentum map, so that the restricted map remains locally surjective.

Proposition 3.1 *Let $(A, B) \in C_1 \times C_2$ be a simultaneously decomposable pair which generates an irreducible group with BA regular elliptic. Then the differential of $\tilde{\mu}_L$ at (A, B) is surjective so that $\tilde{\mu}_L$ is locally surjective at that point.*

Proof. We prove this in a manner analogous to that of the corresponding result when the source is all of $C_1 \times C_2$, but the result is more subtle which makes the proof more difficult. We use again the Lie-algebra formalism developed in [FW1] for the Lagrangian setting. Our starting point is a triple of $\mathbb{R}$-planes L_1, L_2, L_3 with associated $\mathbb{R}$-reflections σ_1, σ_2, σ_3 such that: $A = \sigma_2\sigma_1$ and $B = \sigma_3\sigma_2$ and we study deformations of the conjugacy class of the product $BA = \sigma_3\sigma_1$. We could write down explicitly the tangent space of decomposable pairs inside the product $C_1 \times C_2$, but this is not easy to do. Instead, we will follow the method of [FW1] and investigate an explicit subclass of deformations around a decomposable pair such that these deformations remain decomposable and they sweep all directions in the image. To do this, Falbel and Wentworth introduced two classes of Lagrangian deformations in $U(n)$, which they called *twisting* and *real bending*. The twist deformations are obtained by rotating each Lagrangian plane by a (central) $U(1)$ factor, while the bending deformations are defined by rotating a certain number of the planes by an element which stabilizes one of them (an orthogonal transformation). The twist deformations don't have an obvious analog in the complex hyperbolic setting, whereas the bending deformations can be directly transposed to this case. In fact, the bending deformations will suffice for our purposes; we will focus on those around the $\mathbb{R}$-plane L_2. Precisely, a *real bending about L_2* is a deformation which replaces σ_1, σ_2, σ_3 with σ_1, σ_2, $O\sigma_3O^{-1}$ where O is in the stabilizer O_2 of L_2 in $PU(2,1)$ (a subgroup conjugate to $PO(2,1)$). We will prove the following lemma which implies the statement of the proposition:

Lemma 3.1 *The real bendings about L_2 sweep all possible deformations of the conjugacy class of $BA = \sigma_3\sigma_1$.*

This can be seen by computing the relative positions of the tangent space to the fiber of π and the image of the bending deformations by the differential of μ in the composite map:

$$C_1 \times C_2 \xrightarrow{\mu} G \xrightarrow{\pi} \mathbb{T}^2/\mathfrak{S}_2$$

These subspaces of the tangent space $T_{BA}G$ can be seen in the Lie algebra $\mathfrak{g} = \mathfrak{su}(2,1)$ by right translation by $(BA)^{-1}$.

We will need the following important result (see Prop. 3.1 of [FW1]):

Lemma 3.2 *Let L_i and L_j be two $\mathbb{R}$-planes in $H^2_{\mathbb{C}}$, σ_i and σ_j their associated $\mathbb{R}$-reflections with product $g = \sigma_i\sigma_j$. If O_i, O_j denote the stabilizers of L_i and L_j, $Z(g)$ the centralizer of g in $PU(2,1)$, and $\mathfrak{o}_i$, $\mathfrak{o}_j$, $\mathfrak{z}(g)$ the corresponding Lie algebras, then:*

- *there is an orthogonal decomposition:* $\mathfrak{z}(g) = (\mathfrak{o}_i + \mathfrak{o}_j)^\perp \oplus (\mathfrak{o}_i \cap \mathfrak{o}_j)$
- *if g is regular elliptic:* $\mathfrak{su}(2,1) = \mathfrak{o}_i \oplus \mathfrak{o}_j \oplus \mathfrak{z}(g)$

The first claim is Prop. 3.1 of [FW1]. We derive the second claim (analogous to their Cor. 3.1) by noting that if g is regular elliptic the intersection $\mathfrak{o}_i \cap \mathfrak{o}_j$ is trivial, and that the Killing form is non-degenrate.

Now we can write the deformations of $BA = \sigma_3\sigma_1$ by a real bending around L_2 as paths $O(t)\sigma_3 O(t)^{-1}\sigma_1$ with $O(t) \in O_2$ and $O(1) = Id$. We differentiate this expression and obtain, translating back into $\mathfrak{g}$ by $(BA)^{-1}$ and writing $o = \dot{O}(0)$:

$$(o\sigma_3\sigma_1 - \sigma_3 o\sigma_1)\sigma_1\sigma_3 = (Id - Ad_{\sigma_3})o$$

with $o \in \mathfrak{o}_2$. Thus the image of the vectors tangent to the bending deformations span the subspace $(Id - Ad_{\sigma_3})(\mathfrak{o}_2)$ of $\mathfrak{g}$. Now recall that the tangent space to the fiber of π at the point BA is $Im(Id - Ad_{BA})$. We will have shown the surjectivity of the differential of $\tilde{\mu}_L = \pi \circ \mu_L$ if we prove that the sum of these two subspaces fills the whole tangent space $T_{BA}G$; equivalently we show that their orthogonal complements intersect trivially:

$$((Id - Ad_{\sigma_3})(\mathfrak{o}_2))^\perp \cap Im(Id - Ad_{BA})^\perp = (Id - Ad_{\sigma_3})(\mathfrak{o}_2)^\perp \cap \mathfrak{z}(BA) = \{0\}$$

Indeed, we show successively:

- $z \in (Id - Ad_{\sigma_3})(\mathfrak{o}_2)^\perp \iff (Id - Ad_{\sigma_3})z \in \mathfrak{o}_2^\perp$
- $z \in \mathfrak{z}(BA) \implies (Id - Ad_{\sigma_3})z \in \mathfrak{z}(BA)$
- $\mathfrak{o}_2^\perp \cap \mathfrak{z}(BA) = \{0\}$
- $(Id - Ad_{\sigma_3})z \in \mathfrak{o}_2^\perp \cap \mathfrak{z}(BA)$ and $z \in \mathfrak{z}(BA) \iff z = 0$

The first item is obtained by a computation:

$$\begin{array}{rcl} z \in (Id - Ad_{\sigma_3})(\mathfrak{o}_2)^\perp & \iff & (\forall o \in \mathfrak{o}_2)\ \langle o - Ad_{\sigma_3}o, z\rangle = 0 \\ & \iff & (\forall o \in \mathfrak{o}_2)\ \langle o, z\rangle - \langle Ad_{\sigma_3}o, z\rangle = 0 \\ & \iff & (\forall o \in \mathfrak{o}_2)\ \langle o, z\rangle - \langle o, Ad_{\sigma_3}z\rangle = 0 \\ & \iff & (\forall o \in \mathfrak{o}_2)\ \langle o, z - Ad_{\sigma_3}z\rangle = 0 \end{array}$$

For the second item we compute, for $z \in \mathfrak{z}(BA)$:

$$(Id - Ad_{BA})(z - Ad_{\sigma_3}z) = -(Id - Ad_{BA})Ad_{\sigma_3}z = Ad_{\sigma_3\sigma_1\sigma_3}z - Ad_{\sigma_3}z = Ad_{\sigma_3}(Ad_{(BA)^{-1}}z - z) = 0$$

The third item follows from the above lemma, noting that:

$$\mathfrak{o}_2^\perp \cap \mathfrak{z}(BA) = \mathfrak{o}_2^\perp \cap (\mathfrak{o}_1 \oplus \mathfrak{o}_3)^\perp = (\mathfrak{o}_1 \oplus \mathfrak{o}_2 \oplus \mathfrak{o}_3)^\perp = \{0\}$$

The fourth item is obtained by noting that a $z \in \mathfrak{g}$ which satisfies the left-hand side is both in $\mathfrak{o}_3 = \mathfrak{z}(\sigma_3)$ and in $\mathfrak{o}_1$ which have trivial intersection if BA is regular elliptic. This concludes the proof of the proposition. □

3.1.2 Reducible groups are decomposable

We have just seen that decomposable groups have locally the same image as all elliptic groups near an irreducible. The situation is simpler in the case of reducible groups, which are all decomposable (so that the image is obviously the same).

Proposition 3.2 *Let A and B be two elliptic transformations with a common fixed point in $H^2_{\mathbb{C}}$. Then A and B are simultaneously decomposable.*

This was proven in [FP], theorem 2.1 on p. 224. The result is also valid for hyperbolic reducible groups (generated by two elliptic elements), which fix a point outside of $H^2_{\mathbb{C}}$.

Proposition 3.3 *Let A and B be two elliptic transformations which stabilize a common $\mathbb{C}$-plane. Then A and B are simultaneously decomposable.*

Proof. This is easily seen once we recall the characterization of which $\mathbb{R}$-reflections can appear in a decomposition of an elliptic transformation. Given $g \in PU(2,1)$, we say that an $\mathbb{R}$-plane L *decomposes* g if there is a decomposition $g = \sigma\sigma'$ where σ is the $\mathbb{R}$-reflection in L and σ' is another $\mathbb{R}$-reflection. We have proven in [FP] (see Proposition 4 on p. 223) that:

- if g is a complex reflection in a point, then any $\mathbb{R}$-plane through its fixed point decomposes g.
- if g is a $\mathbb{C}$-reflection then any $\mathbb{R}$-plane intersecting its mirror in a geodesic decomposes g.
- if g is regular elliptic, it stabilizes exactly two $\mathbb{C}$-planes (which contain its fixed point). Then an $\mathbb{R}$-plane decomposes g if and only if it passes through its fixed point and interects each of these $\mathbb{C}$-planes in a geodesic.

Now the proposition is obvious because if A and B stabilize a common $\mathbb{C}$-plane it suffices to consider an $\mathbb{R}$-plane containing the geodesic in this $\mathbb{C}$-plane joining the fixed points of A and B if they are both regular elliptic (the other cases are even easier) to see that A and B are simultaneously decomposable. □

3.1.3 Local convexity around the totally reducible vertices

All the results of the analogous section on elliptic triangle groups remain valid, because all of our arguments (and computations) were based on reducible groups.

3.2 A Lagrangian obstruction

There is a condition on the pairs of angles of a triple of $\mathbb{R}$-planes which intersect pairwise inside $H^2_{\mathbb{C}}$ coming from the fact that the Riemannian angle between two geodesics, each in an $\mathbb{R}$-plane, is bounded by the angle pair as follows (see propositions 1.2.2 and 1.2.3 of [P]):

Proposition 3.4 *Let L_1 and L_2 be two intersecting $\mathbb{R}$-planes with angle pair $\{\theta_1, \theta_2\}$ ($\theta_i \in [0, \pi[$) and let $g_1 \subset L_1$, $g_2 \subset L_2$ be two intersecting geodesics, with Riemannian angle $\lambda \in [0, \pi[$. Then the following inequality holds:*

$$\text{Min}\{\theta_1, \theta_2, \pi - \theta_1, \pi - \theta_2\} \leqslant \lambda \leqslant Max\{\theta_1, \theta_2, \pi - \theta_1, \pi - \theta_2\}$$

Recall that a characteristic feature of non-positive curvature (not necessarily constant, see [BGS] p. 6) is that the sum of Riemannian angles in a geodesic triangle is less than π. This fact, combined with the above proposition, gives us the following condition in a Lagrangian triangle:

Proposition 3.5 *Let L_1, L_2, L_3 be three pairwise intersecting $\mathbb{R}$-planes with angle pairs $\{\theta_1, \theta_2\}$, $\{\theta_3, \theta_4\}$, $\{\theta_5, \theta_6\}$ ($\theta_i \in [0, \pi[$). Then the following inequality holds:*

$$\sum_{i=1,3,5} \text{Min}\{\theta_i, \theta_{i+1}, \pi - \theta_i, \pi - \theta_{i+1}\} < \pi$$

Now if as before we fix the two first angle pairs $\{\theta_1, \theta_2\}$, $\{\theta_3, \theta_4\}$ and look at the possible values for $\{\theta_5, \theta_6\}$, two possibilities can occur, according to the values of

$$\alpha = \text{Min}\{\theta_1, \theta_2, \pi - \theta_1, \pi - \theta_2\} \text{ and } \beta = \text{Min}\{\theta_3, \theta_4, \pi - \theta_3, \pi - \theta_4\} :$$

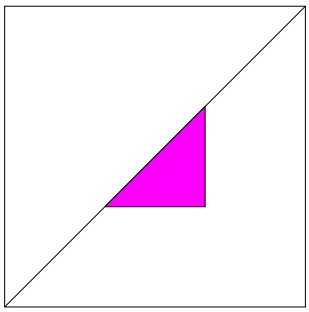

Figure 11: Obstruction in a Lagrangian triangle

- If $\alpha + \beta < \frac{\pi}{2}$ there is no constraint on $\{\theta_5, \theta_6\}$, because we always have:
$$\text{Min}\{\theta_5, \theta_6, \pi - \theta_5, \pi - \theta_6\} \leqslant \frac{\pi}{2}.$$
- If $\alpha + \beta \geqslant \frac{\pi}{2}$ then $\{\theta_5, \theta_6\}$ must satisfy the inequality:
$$\text{Min} = \{\theta_5, \theta_6, \pi - \theta_5, \pi - \theta_6\} < \pi - \alpha - \beta$$

This condition forbids a triangular region of $\mathbb{T}^2/\mathfrak{S}_2$ near the middle of the diagonal, as in figure 11. Compare with the analysis of which parts of the diagonal were attained in section 2.6.

4 An example: polygons containing Mostow's lattices $\Gamma(p, t)$

4.1 The configuration polygon

We consider a degenerate case where at least one of the generators is a complex reflection (one angle is zero) or a complex reflection in a point (two equal angles); these cases do not exactly fit in the generic description which we have given, so that we describe them here in detail. In fact in all these cases (except the non-convex case of two $\mathbb{C}$-reflections) we can prove that the image is exactly the locally convex hull of the reducibles. The result is the following:

Proposition 4.1 *If one of the generators A or B is a complex reflection (resp. in a point) then the image of the momentum map is exactly the locally convex hull of the reducible walls. In particular, if W_{red} is connected in the affine chart, then the image is a convex polygon. Moreover, for each point on the boundary of the square which is in the image but not reducible, the product AB is parabolic.*

Recall that in general we do not know whether the latter points (with angles $\{0, \theta\}$) represent parabolic elements or complex reflections.

Proof. The argument is the same for both claims; it is simply the fact that if A or B is special elliptic (a complex reflection or a complex reflection in a point) and if AB is also special elliptic, then the group is reducible. Indeed, these two motions then each fix pointwise a complex line of $\mathbb{C}P^2$, and these lines must intersect in $\mathbb{C}P^2$. Thus all chambers touching the diagonal at more than a reducible point are excluded. □

A case of particular interest is the case of one complex reflection, since it contains the case which originally motivated this work, that of Mostow's lattices $\Gamma(p, t)$ (see [M1], [M2] and figures 12 and 15). We go into this example in more detail, in the hope of finding new discrete groups in the pictures.

The reducible configuration now consists in the spherical reducible segment together with two non-degenerate hyperbolic reducible segments (one at each vertex); as before we know that the whole image is exactly the convex hull of the reducibles (see figure 12). In the figure we have also featured a segment inside the polygon which represents Mostow's one-parameter family of lattices $\Gamma(p, t)$ (here, each integer value of p corresponds to a different picture). We will focus on the case of $\Gamma(3, t)$ in the last section (in our notation, this is a segment inside the image for pairs $\{\frac{2\pi}{3}, \frac{4\pi}{3}\}$, $\{0, \frac{2\pi}{3}\}$).

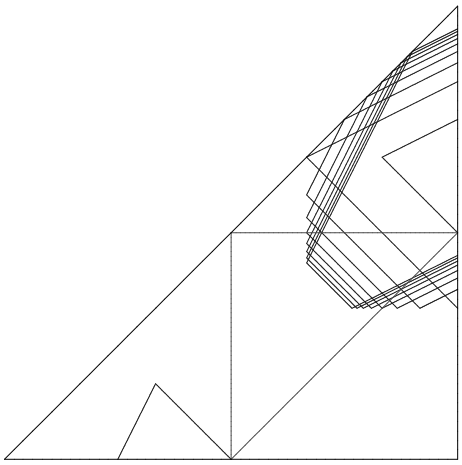

Figure 12: The picture for angle pairs $\{\frac{2\pi}{3}, \frac{4\pi}{3}\}$, $\{0, \frac{2\pi}{p}\}$ for $p = 2, 3, ..., 10$; the central triangle represents Mostow's family $\Gamma(p, t)$ (see enlargement for $p = 3$ in figure 15).

4.2 The search for discrete groups

There is an obvious condition that a subgroup of $PU(2, 1)$ must satisfy in order to be discrete (as in any Lie group acting on a space with compact point stabilizers), namely that elements in this subgroup which fix a point must be of finite order. For an elliptic element in $PU(2, 1)$, this means that both of its angles are rational multiples of π; in fact it is often safer to ask for integer fractions of 2π (or for pairs of the type $\{\frac{2\pi}{n}, \frac{2k\pi}{n}\}$) for some generators if we hope for Poincaré-type tessellation conditions. Our setting is well adapted to this simple idea because we can simultaneously control the angles of the generators A, B and of their product. However, this only indicates what might be some interesting candidates for discrete groups or lattices, and there remains the difficult question of deciding whether or not a given group (defined by two matrix generators) is discrete.

A first difficulty is then to choose a place to start looking; we have chosen as a first step to further investigate some cases where lattices or discrete groups were previously known to exist. For the time being, we have only begun the search in the case of Mostow's lattices $\Gamma(3, t)$ (this will appear in [PP]). This case is not typical because one of the generators is a $\mathbb{C}$-reflection, so that there are no fibers: each point of the image of $\tilde{\mu}$ (a triangle) corresponds to a single group (up to conjugacy).

We will focus on the groups introduced by Mostow in his 1980 paper ([M1]), which he denoted $\Gamma(p, t)$ (where $p = 3, 4, 5$ and t is a real parameter); note however that this description also includes, for larger integer values of p, 22 of the 27 Picard lattices (also known as the Deligne-Mostow lattices of dimension 2), as described in detail in his subsequent paper [M2].

We will only decribe briefly the construction of these groups, for which we refer to (the original paper or) [DFP]. The group $\Gamma(p, t)$ is generated by three braiding complex reflections of order p (R_1,R_2, and R_3) which are permuted by a cyclic element J. We consider as in [DFP] not exactly $\Gamma(p, t)$ but the sometimes bigger group $\tilde{\Gamma}(p, t)$ generated by R_1 and J (it contains $\Gamma(p, t)$ with index 1 or 3). We have noticed that these two generators are decomposed into $\mathbb{R}$-reflections in the following way (with the notation from [DFP]):

$$\begin{cases} J &= \sigma_{12}\sigma_{23} \\ R_1 &= \sigma_{23}\tau \end{cases}$$

The elliptic motions R_1 and J have respective angle pairs $\{0, \frac{2\pi}{p}\}$ and $\{\frac{2\pi}{3}, -\frac{2\pi}{3}\}$. A computation using the explicit form for these matrices tells us that the product $JR_1 = \sigma_{12}\tau$ is semisimple with eigenvalues $-\eta i\overline{\phi} = e^{i\pi(1+1/p+1/2-t/3)}$ and $\pm\sqrt{-\eta i\phi} = \pm e^{i\pi(1+1/p+1/2+t/3)/2}$ where $\eta = e^{i\pi/p}$ and $\phi = e^{i\pi t/3}$. Thus it is elliptic and its angles are given by dividing the two eigenvalues of positive type by that of negative type, which is here (by a tedious computation) $-e^{i\pi(1+1/p+1/2+t/3)/2}$. We obtain for JR_1 the angle pair $\{\pi, \frac{\pi}{2}(\frac{1}{p} - \frac{1}{2} - t)\}$ (note that $(JR_1)^2$ is a complex reflection). The angles in the Lagrangian triple are obtained by dividing all of these by two; this gives us the diagram of figure 13.

We now consider the case $p = 3$ and see how the family $\tilde{\Gamma}(p, t)$ fits into the picture of the momentum

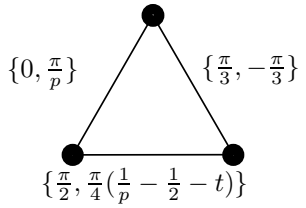

Figure 13: Diagram of $\mathbb{R}$-reflections for $\tilde{\Gamma}(p,t)$

t	0	$\frac{1}{30}$	$\frac{1}{18}$	$\frac{1}{12}$	$\frac{5}{42}$	$\frac{1}{6}$	$\frac{7}{30}$	$\frac{1}{3}$
$-\frac{1}{\pi}\cdot$Angle of JR_1	$\frac{1}{12}$	$\frac{1}{10}$	$\frac{1}{9}$	$\frac{1}{8}$	$\frac{1}{7}$	$\frac{1}{6}$	$\frac{1}{5}$	$\frac{1}{4}$
$-\frac{1}{\pi}\cdot$Angle of R_1J^{-1}	$\frac{1}{12}$	$\frac{1}{15}$	$\frac{1}{18}$	$\frac{1}{24}$	$\frac{1}{42}$	0	$-\frac{1}{30}$	$-\frac{1}{12}$

Figure 14: The discrete groups $\Gamma(3,t)$

polygon associated to angle pairs $\{0, \frac{2\pi}{p}\}$ and $\{\frac{2\pi}{3}, -\frac{2\pi}{3}\}$. This gives us the segment of figure 12, which we will now enlarge in order to see the points corresponding to lattices (see figure 15). Note that this segment is characterized by the fact that R_1 and its two conjugates R_2 and R_3 satisfy a braiding relation of order 3 (namely, $R_iR_jR_i = R_jR_iR_j$). There are 8 values of the parameter t which yield lattices, listed in the table of figure 14 along with the corresponding values of the (non-trivial) rotation angle of JR_1.

An important thing to note is that this angle is closely related to one of the two conditions (the Picard integrality conditions, see [DFP]) which ensure the discreteness of the group. Recall that these conditions come from the analysis of only two conjugacy classes of $\mathbb{C}$-reflections in the group, namely those of R_2R_1J and $J^{-1}R_1R_2$; their rotation angle must be an integer fraction of 2π if the group is to be discrete, and it turns out that these two conditions suffice. Now the former of these conjugacy classes contains $(R_1J^{-1})^2$ and the latter contains $(JR_1)^2$, because $R_2 = JR_1J^{-1}$ so that:

$$R_2R_1J = JR_1J^{-1}R_1J = J(R_1J^{-1}R_1J^{-1})J^{-1} \text{ and } J^{-1}R_1R_2 = J^{-1}R_1JR_1J^{-1} = J(JR_1JR_1)J^{-1}$$

This means that one of the two discreteness conditions is immediately visible on our picture: the angle of JR_1 which depends on the parameters must be an even integer fraction of 2π. In fact the second condition also fits in the same picture, because it so happens that J^{-1} is conjugate to J, so that the angles of R_1J^{-1} are contained in the same picture (but correspond to different points). The value of the (non-trivial) rotation angle of R_1J^{-1} in the 8 discrete groups is also listed in table 14; the corresponding points of the picture are in the same segment as the previous ones, but to their right. This is an example of different points in the same picture which yield conjugate subgroups of $PU(2,1)$; this situation only becomes worse if we worry about commensurability classes of subgroups. In fact this simple idea of exchanging two among the four fundamental classes of $\mathbb{C}$-reflections is behind the isomorphisms and commensurabilities among lattices discovered by Sauter (see [Sa]) and further investigated in the book of Deligne and Mostow (see [DM]).

Recall from proposition 4.1 the complete description of the momentum polygon in this case (angles $\{0, \frac{2\pi}{3}\}$ and $\{\frac{2\pi}{3}, -\frac{2\pi}{3}\}$). The polygon is the triangle of figures 12 and 15, bounded by a spherical reducible segment, a hyperbolic reducible segment, and the "boundary segment" $[2\pi, \theta]$ for $\theta \in [\frac{2\pi}{3}, \frac{5\pi}{3}]$ which comprises parabolic conjugacy classes (except at its endpoints).

References

[A] M. F. Atiyah; *Convexity and commuting Hamiltonians*. Bull. London Math. Soc. **14(1)** (1982), 1–15.

[AMM] A. Alekseev, A. Malkin, E. Meinrenken; *Lie group valued moment maps*. J. Diff. Geom. **48(3)** (1998), 445–495.

[AW] S. Agnihotri, C. Woodward; *Eigenvalues of products of unitary matrices and quantum Schubert calculus*. Math. Res. Lett. **5(6)** (1998), 817–836.

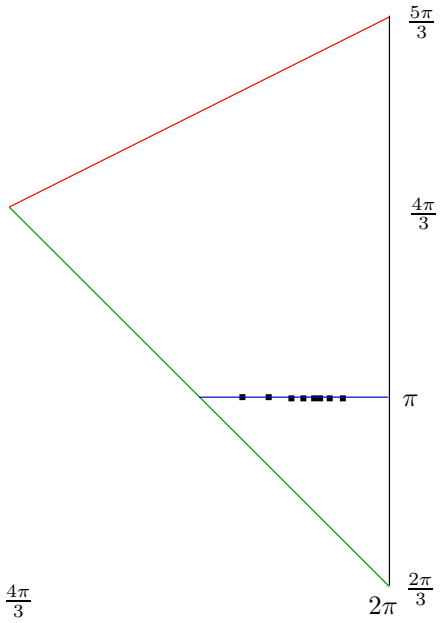

Figure 15: Mostow's groups $\tilde{\Gamma}(p,t)$ inside the momentum polygon

[BGS] W. Ballmann, M. Gromov, V. Schroeder; Manifolds of Nonpositive Curvature. Birkhaüser Progress in Math. vol. 61, 1985.

[Be] P. Belkale; *Local systems on $P^1 - S$ for S a finite set*. Compositio Math. **129(1)** (2001), 67–86.

[Bi1] I. Biswas; *A criterion for the existence of a parabolic stable bundle of rank two over the projective line*. Internat. J. Math. **9(5)** (1998), 523–533.

[Bi2] I. Biswas; *On the existence of unitary flat connections over the punctured sphere with given local monodromy around the punctures*. Asian J. Math. **3(2)** (1999), 333–344.

[DFP] M. Deraux, E. Falbel, J. Paupert; *New constructions of fundamental polyhedra in complex hyperbolic space*. Acta Math. **194** (2005), 155–201.

[DM] P. Deligne, G. D. Mostow; Commensurabilities among lattices in $PU(1,n)$. Annals of Mathematics Studies **132**. Princeton University Press (1993).

[FMS] E. Falbel, J.-P. Marco, F. Schaffhauser; *Classifying triples of Lagrangians in a Hermitian vector space*. Topology Appl. **144** (2004), 1–27.

[FP] E. Falbel, J. Paupert; *Fundamental domains for finite subgroups in $U(2)$ and configurations of Lagrangians*. Geom. Dedicata **109** (2004), 221–238.

[FW1] E. Falbel, R. Wentworth; *Eigenvalues of products of unitary matrices and Lagrangian involutions*. Topology **45** (2006), 65–99.

[FW2] E. Falbel, R. Wentworth; *Produits d'isométries d'un espace symétrique de rang un et compacité à la Mumford-Mahler*. Preprint 2006.

[F] W. Fulton; *Eigenvalues, invariant factors, highest weights, and Schubert calculus*. Bull. Amer. Math. Soc. **37(3)** (2000), 209–249.

[G] W.M. Goldman; Complex Hyperbolic Geometry. Oxford Mathematical Monographs. Oxford Science Publications (1999).

[GS1] V. Guillemin, S. Sternberg; *Convexity properties of the moment mapping*. Invent. Math. **67(3)** (1982), 491–513.

[GS2] V. Guillemin, S. Sternberg; *Convexity properties of the moment mapping II*. Invent. Math. **77(3)** (1984), 533–546.

[Kl1] A. Klyachko; *Stable bundles, representation theory and Hermitian operators*. Selecta Math. (NS) **4(3)** (1998), 419–445.

[Kl2] A. Klyachko; *Vector bundles, linear representations, and spectral problems*. Proceedings of the International Congress of Mathematicians, Vol. II (Beijing, 2002), 599–613, Higher Ed. Press, Beijing (2002).

[Ko] V. P. Kostov; *The Deligne-Simpson problem–a survey*. J. Algebra **281** (2004), 83–108.

[M1] G. D. Mostow; *On a remarkable class of polyhedra in complex hyperbolic space*. Pacific J. Math. **86** (1980), 171–276.

[M2] G. D. Mostow; *Generalized Picard lattices arising from half-integral conditions*. Publ. Math. IHES **63** (1986), 91–106.

[PP] J. R. Parker, J. Paupert; *Unfaithful complex hyperbolic triangle groups II: Higher order reflections*. In preparation.

[P] J. Paupert; Configurations of Lagrangians, fundamental domains and discrete subgroups of $PU(2,1)$. Ph.D. Thesis, Université Paris 6 (2005).

[Sa] J. K. Sauter; *Isomorphisms among monodromy groups and applications to lattices in* $PU(1,2)$. Pacific J. Math. **146(2)** (1990), 331–384.

[Sf] F. Schaffhauser; Decomposable representations and Lagrangian submanifolds of moduli spaces associated to surface groups. Thesis, Université Paris 6, 2005.

[Sz] R. E. Schwartz; *Complex hyperbolic triangle groups*. Proceedings of the International Congress of Mathematicians, Vol. II (Beijing, 2002), 339–349, Higher Ed. Press, Beijing, 2002.

[W1] A. Weinstein; *Poisson geometry of discrete series orbits, and momentum convexity for noncompact group actions*. Lett. Math. Phys. **56(1)** (2001), 17-30.

[W2] A. Weinstein; *The geometry of momentum*. Preprint, arXiv:math.SG/0208108 (2002).